Enhancing quality inspection efficiency and reliability of unscreened recycled coarse aggregates (RCA) streams using innovative mobile sensor-based technology

Chang, Cheng; Di Maio, Francesco; Bheemireddy, Rajeev; Posthoorn, Perry; Gebremariam, Abraham T.; Rem, Peter

DOI
10.1016/j.dibe.2025.100611

Publication date
2025

Document Version
Final published version

Published in
Developments in the Built Environment

Citation (APA)
Chang, C., Di Maio, F., Bheemireddy, R., Posthoorn, P., Gebremariam, A. T., & Rem, P. (2025). Enhancing quality inspection efficiency and reliability of unscreened recycled coarse aggregates (RCA) streams using innovative mobile sensor-based technology. *Developments in the Built Environment*, *21*, Article 100611. https://doi.org/10.1016/j.dibe.2025.100611

Developments in the Built Environment 21 (2025) 100611

Contents lists available at ScienceDirect

Developments in the Built Environment

journal homepage: www.sciencedirect.com/journal/developments-in-the-built-environment

Enhancing quality inspection efficiency and reliability of unscreened recycled coarse aggregates (RCA) streams using innovative mobile sensor-based technology

Cheng Chang [a,*], Francesco Di Maio [a], Rajeev Bheemireddy [b], Perry Posthoorn [b], Abraham T. Gebremariam [a], Peter Rem [a]

[a] Resource & Recycling, Department of Engineering Structures, Faculty of Civil Engineering and Geosciences, Delft University of Technology, Stevinweg 1, 2628 CN, Delft, the Netherlands
[b] DEMO, Delft University of Technology, Gebouw 36, Mekelweg 4, 2628 CD, Delft, the Netherlands

ARTICLE INFO

Keywords:
Recycled coarse aggregates (RCA)
Quality inspection
Concrete recycling
Conveyor belt
3D scanner gocator
Laser-induced breakdown spectroscopy (LIBS)

ABSTRACT

Recycled coarse aggregates (RCA) from End-of-Life (EoL) concrete face resistance due to inconsistent quality. To address this, a mobile, containerized sensor-based inspection system is developed, capable of processing over 100 tons of RCA per hour. Using advanced 3D scanning and laser-induced breakdown spectroscopy (LIBS), the system ensures reliable real-time analysis of particle size distribution (PSD) (Root Mean Square Error: <5.5%) and contaminant detection (Accuracy: 0.94). Incremental learning techniques dynamically update chi-square distribution parameters as new spectral data becomes available, refining models continuously without full retraining and sustaining high classification performance. Monitoring data are recorded on radio frequency identification (RFID) tags, enhancing traceability. This innovation improves efficiency compared to traditional methods, supporting sustainable practices in the construction industry. Its applications also extend to related fields such as mining, waste management, and resource recovery, contributing to the circular economy, reducing reliance on natural aggregates, and promoting environmentally friendly infrastructure development.

1. Introduction

The growing global population and rapid urbanization have significantly increased the generation of Construction and Demolition Wastes (CDWs), making their management a critical challenge for the construction industry (Aslam et al., 2020; Kabirifar et al., 2020). CDWs are among the largest waste streams globally, comprising diverse materials such as concrete, wood, metal, and plastics (Galán et al., 2019; Soto-Paz et al., 2023). Inefficient handling and improper disposal of these wastes not only accelerate environmental degradation but also deplete natural resources, emphasizing the urgent need for sustainable waste management solutions (Akhtar and Sarmah, 2018; Amesho et al., 2023; K. Zhang et al., 2023). In response to these challenges, many countries have implemented recycling and reuse strategies to reduce the environmental footprint of CDWs and conserve valuable resources (Lederer et al., 2020; Luciano et al., 2022; Su et al., 2024). One promising approach involves the recycling of concrete from End-of-Life (EoL) infrastructures to produce recycled coarse aggregates (RCA), which serve as substitutes for natural aggregates. The increasing demand for construction materials, alongside the urgency for sustainable waste management, has propelled this practice as a progressively feasible solution. This practice enables resource conservation, reduces environmental impact, and supports the circular economy (Gálvez-Martos et al., 2018; C. Zhang et al., 2022). This transition aligns with global circular economy initiatives and highlights the construction industry's shift towards more sustainable practices.

Recognizing the potential environmental detriments and the associated carbon footprint of unfettered natural aggregate extraction, many countries are promoting sustainable practices in the construction domain (Al Martini et al., 2023; Aslam et al., 2020; Kabirifar et al., 2020; Sai Trivedi et al., 2023; Soto-Paz et al., 2023). The European Union (EU) has distinctly emerged as a frontrunner, adeptly incorporating sustainable recycling methodologies into mainstream construction practices (Akhtar and Sarmah, 2018; Gálvez-Martos et al., 2018; Lederer et al.,

This article is part of a special issue entitled: Novel Materials Testing published in Developments in the Built Environment.

* Corresponding author.
E-mail addresses: chang-cheng@outlook.com, C.Chang-1@tudelft.nl (C. Chang).

https://doi.org/10.1016/j.dibe.2025.100611
Received 22 August 2024; Received in revised form 4 January 2025; Accepted 20 January 2025
Available online 24 January 2025

2020; Marique and Rossi, 2018; C. Zhang et al., 2022). This shift is not merely a reaction to environmental urgency, it marks a strategic transition towards resource conservation and a reduced carbon footprint for the entire construction sector.

However, the transition to RCA is fraught with challenges, chiefly concerning the assurance of their quality and purity (J. Kim, 2022; H. Wu et al., 2023). These challenges are accentuated when the RCA is sourced from a diverse range of dismantled infrastructures, bringing to the fore issues related to the presence and detection of contaminants (Alaejos et al., 2013). These contaminants, if not properly identified and managed, can significantly compromise the integrity and applicability of RCA in new construction projects (Poon and Chan, 2007; L. Wu et al., 2024). Consequently, addressing these quality-related concerns is critical to maintaining the performance, durability, and reliability of RCA-infused construction (Marín-Cortés et al., 2024; Vegas et al., 2015). It requires a focused approach towards standardizing the quality assessment methods and developing stringent guidelines to ensure that the recycled aggregates meet or surpass the performance metrics of their natural counterparts.

Historically, the assessment of RCA primarily relied on traditional methodologies, characterized by their labor-intensive nature, prolonged time frames, and manual procedures (Marie and Mujalli, 2019; Tuan et al., 2022). While these methods have served the industry for a significant period, their inherent limitations, such as potential imprecisions and inefficiencies, have become increasingly evident as the construction sector has progressed. Specifically, traditional methods for RCA quality control, such as manual sieving and inspection, face several critical challenges: (1) low accuracy: manual methods are prone to human error, resulting in inconsistent assessments; (2) inefficiency: labor-intensive processes are time-consuming and unsuitable for high-throughput applications; (3) lack of real-time feedback: traditional methods do not provide immediate insights, delaying necessary adjustments in production lines; and (4) limited adaptability: these methods struggle to operate effectively in dynamic environments such as demolition sites. As the industry's aspirations continue to shift towards achieving enhanced operational efficiencies without compromising quality, the imperative for a more innovative, efficient, and precise quality inspection mechanism has grown more pronounced.

Amidst the prevailing challenges, the emergence of sensor technology provides a promising solution (Barri et al., 2020; Cabral et al., 2023; Chang, 2025; Chang et al., 2022, 2025; Lotfi et al., 2015; Trotta et al., 2021; Xia and Bakker, 2014). The rising demand underscores the potential of recent advancements in sensor technology (Bonifazi et al., 2018; Nalon et al., 2022; Vegas et al., 2015), which offer real-time, on-site characterization of RCA. Such state-of-the-art methodologies not only enable prompt feedback, expediting the decision-making

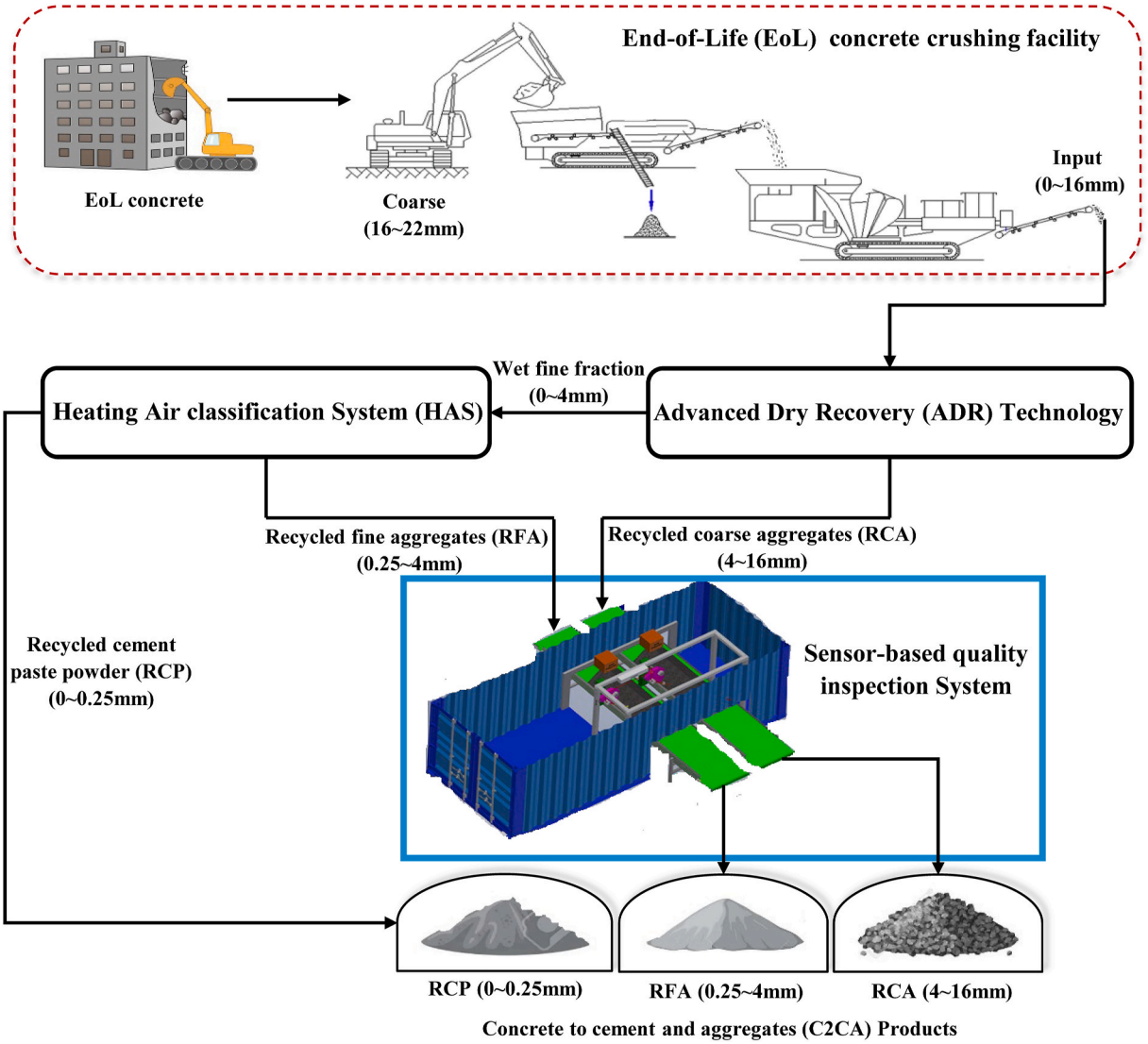

Fig. 1. Concrete to Cement and Aggregate (C2CA) technology.

process and any necessary recalibrations in production but also augment the overall efficiency of the RCA production and usage cycle. Furthermore, the integration of real-time sensors into the RCA assessment process signifies more than just technological evolution, it represents a broader shift towards sustainable construction practices. By allowing for instant feedback and adjustments, these systems can reduce wastage, optimize resource use, and ensure that the resulting product meets the necessary quality benchmarks.

This research delves into the sensor-based quality inspection system integrated into the Concrete to Cement and Aggregate (C2CA) technology (Fig. 1). Fig. 2 presents a flowchart summarizing the methodological steps of the quality inspection. This quality inspection system employs a 3D scanner Gocator and a laser-induced breakdown spectroscopy (LIBS) sensor to provide a comprehensive granulometric analysis of RCA and enable potential contaminants. The accuracy and validity of the particle size distribution (PSD) measurement method are verified using 3D modeling with X-ray tomography, comparable to traditional manual sieving. Additionally, incremental learning techniques update existing models as new spectral data becomes available, dynamically adjusting chi-square distribution parameters. This approach ensures continuous model refinement without the need for complete retraining, enhancing computational efficiency and sustaining high classification performance.

To overcome the challenges posed by traditional quality control methods, this mobile sensor-based system offers significant advantages:

(1) Real-Time Precision: LIBS achieves consistent contaminant detection under dynamic and static conditions with an accuracy of 94%, and PSD estimation shows a Root Mean Square Error of less than 5.5%.
(2) High Throughput and Scalability: Capable of processing over 100 tons of RCA per hour, the system supports industrial-scale operations, meeting the demands of large-scale construction and demolition projects.
(3) Dynamic Adaptability: Incremental learning ensures the model dynamically updates with new spectral data, eliminating the need for full retraining and maintaining robust performance.
(4) Mobility and Versatility: The containerized design enables on-site operation, reducing transportation costs, optimizing resource allocation, and enhancing efficiency in diverse demolition contexts.

The innovative use of advanced sensors enables real-time assessments on-site, which is particularly valuable in the dynamic context of demolition sites. By examining operational aspects and evaluating effectiveness in real-world scenarios, this research aims to highlight how this technology could improve the quality assessment of RCA. Through experimentation and analysis, the study emphasizes the advancements in RCA processing, presenting a pathway for industries to achieve sustainable growth while maintaining high-quality standards.

2. Materials and methods

2.1. Material samples

This study used recycled concrete aggregates obtained from discarded concrete, collected during the dismantling of various infrastructures throughout the Netherlands. To maintain the purity of the EoL concrete, selective demolition methodologies were employed. Additionally, other demolition residuals such as brick, foam, glass, gypsum, mineral fibers, plastics, and wood were manually separated from the collection sites. This segregation process aimed to preserve the integrity of the samples. The primary components of the materials used in this study are detailed in Table 1.

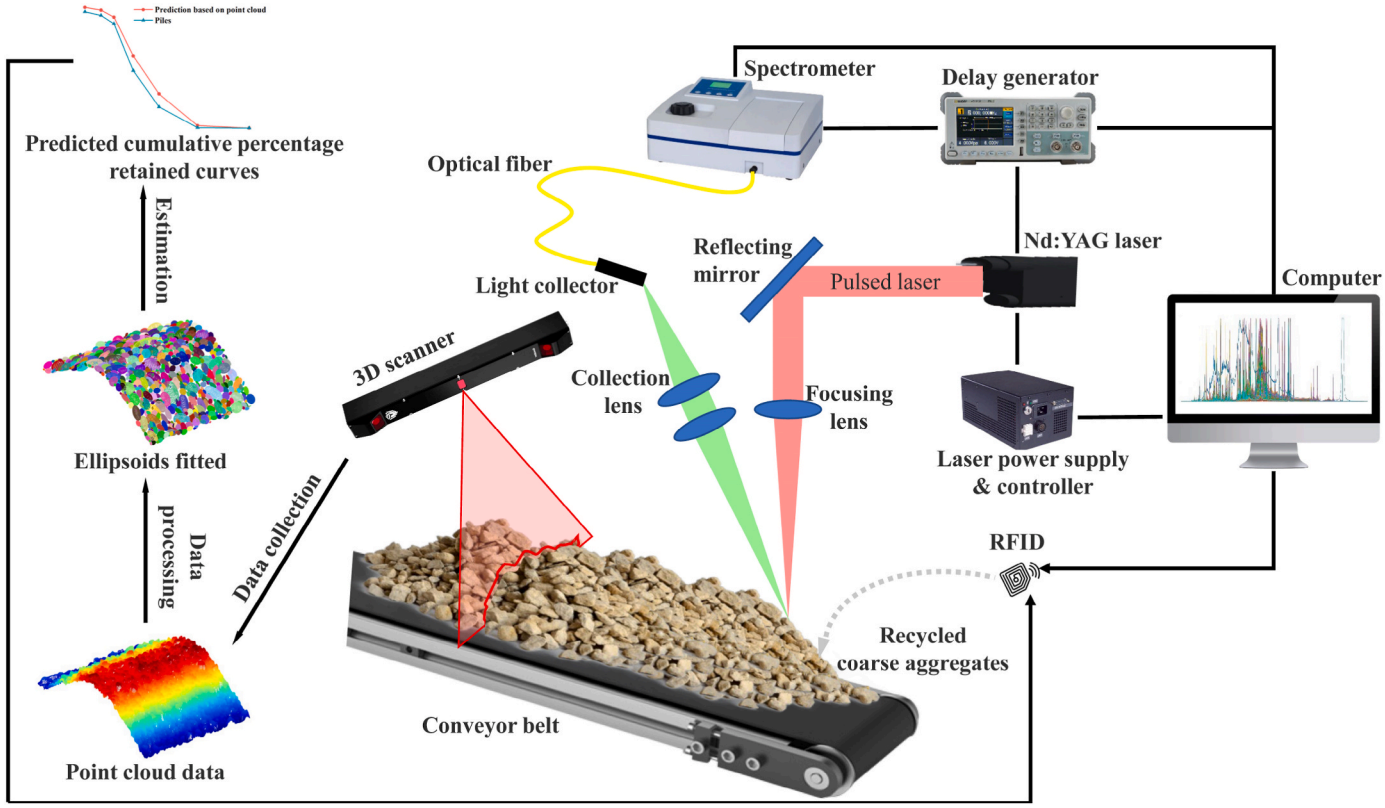

Fig. 2. Schematic of quality inspection process.

Table 1
Principal components for each material.

Material Type	Principal Components
Recycled Coarse Aggregates (RCA)	Silica (SiO_2), Calcium Carbonate ($CaCO_3$), Calcium Silicate Hydrate (C-S-H), Aluminum Oxide (Al_2O_3)
Brick	Silica (SiO_2), Aluminum Oxide (Al_2O_3), Iron Oxide (Fe_2O_3)
Foam	Expanded Polystyrene ((C_8H_8)n), Blowing Agent (C_5H_{12})
Glass	Silica (SiO_2), Sodium Oxide (Na_2O), Calcium Oxide (CaO)
Gypsum	Calcium Sulfate Dihydrate ($CaSO_4 \cdot 2H_2O$)
Mineral Fibers	Silica (SiO_2), Calcium Oxide (CaO), Magnesium Oxide (MgO), Aluminum Oxide (Al_2O_3), Iron(III) Oxide (Fe_2O_3)
Plastics	Polyvinyl Chloride ((C_2H_3Cl)n)
Wood	Cellulose (($C_6H_{10}O_5$)n), Hemicellulose ($C_5H_8O_4$), Lignin ($C_9H_{10}O_3$)
Recycled Cement Paste (RCP)	Calcium Silicate Hydrate (C-S-H), Calcium Hydroxide ($Ca(OH)_2$), Ettringite ($Ca_6Al_2(SO_4)_3(OH)_{12} \cdot 26H_2O$), Calcium Carbonate ($CaCO_3$)
Recycled Fine Aggregates (RFA)	Silica (SiO_2), Calcium Carbonate ($CaCO_3$), Residual Cement Paste (C-S-H, $Ca(OH)_2$)

2.2. Sensor-based quality inspection system

2.2.1. Containerization

The sensor-based quality inspection system, depicted in Fig. 3, plays a critical role in the C2CA technology framework. Housed within a specialized container, this system performs several vital functions.

The container is partitioned into two areas: an inspection room and a control room. These sections are separated to prevent any potential harm to operators from the lasers used during the inspection process. The inspection room is equipped with sensors for material analysis, and it includes a vacuum system designed to reduce dust levels inside the inspection room. Reducing dust is essential, as it enhances the sensors' accuracy by lessening their interference with dust particles. The control room is set up to receive and process various data collected in real-time. It also uses a monitoring system to oversee activities within the inspection room to ensure operational safety and efficiency.

One of the primary advantages of the container is its mobility, which allows easy transport to various demolition sites. This mobility increases operational flexibility and optimizes resource allocation. The container is designed to facilitate the on-site recycling and testing of concrete directly at demolition sites. By processing the demolished concrete on-site, the need to transport it to a remote facility is eliminated. This not only reduces the costs associated with transportation but also minimizes the overall expenses related to the recycling process, as the material is reused or repurposed immediately without additional handling or processing steps.

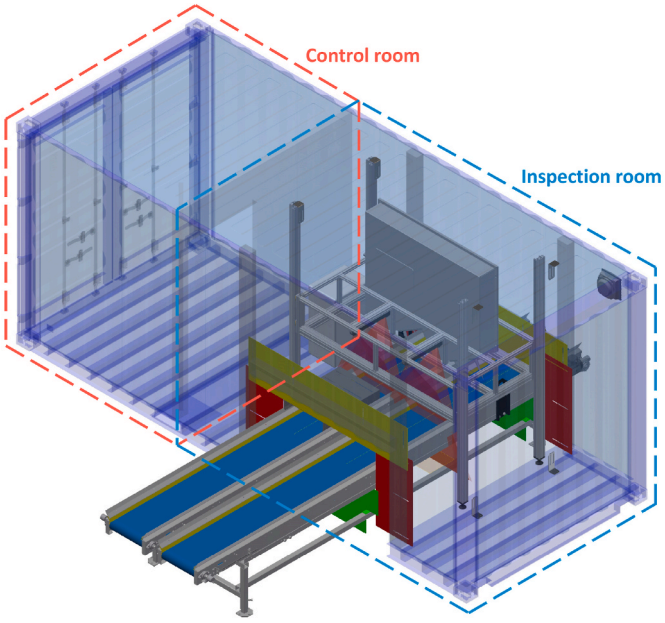

Fig. 3. Sensor-based quality inspection system.

Additionally, the container acts as a protective shield against adverse weather conditions, ensuring the system's functionality despite external environmental challenges. This safeguard is crucial for maintaining the accuracy of the sensors' measurements by protecting the sensitive equipment from damage. Furthermore, beyond its role in adverse weather conditions, the container's presence demonstrates the system's adaptability in different field conditions. Such adaptability not only ensures the reliability of data but also strengthens the overall robustness, resilience, and effectiveness. Consequently, it expands the applicability of the system across various demolition and recycling contexts.

In summary, the containerized setup is fundamental in preserving data integrity, enhancing operational flexibility, and ensuring the system's adaptability. These attributes are key to the technology's effectiveness in a variety of demolition scenarios.

2.2.2. Composition

The sensor-based quality inspection system (Fig. 4) comprises two primary sensors: a 3D scanner Gocator and a LIBS sensor. Both sensors are positioned directly above the conveyor belt. The Gocator specializes in the granulometric analysis of RCA, pinpointing/measuring their PSD. This device is adept at generating high-resolution, three-dimensional point cloud data, capturing detailed information about the surface topology and granular distribution.

The LIBS sensor (Fig. 5) plays a crucial role in identifying contaminant compositions embedded within the RCA. It achieves this by focusing ultra-short pulse lasers on the sample's surface to create plasma, subsequently analyzing the emitted light spectrum from the plasma to determine the material composition and content of the sample. Specific experimental parameters used in this study are detailed in Table 2.

To mitigate interference caused by continuous laser-induced plasma radiation, the detection system employed a time-resolved spectral acquisition method using temporal gating. This technique isolates the emission from the plasma at its peak intensity, typically occurring within the first 20 ns post-laser excitation. A gated detector synchronized with the laser pulses was used to collect only the desired spectral data while excluding background radiation.

To prevent the loss of spectral information during high-speed LIBS operations, several strategies were implemented:

(1) Optimized Laser Focus and Alignment: The laser was precisely focused on the sample surface using the lens with a focal length of 300 mm. This ensured consistent plasma generation, avoiding irregularities in the spectral data.
(2) High-Resolution Spectrometer: The LIBS system employed a spectrometer with a resolution of 0.1 nm, capable of capturing subtle variations in plasma emission.
(3) Temporal Gating: A temporal gate was applied to collect only the most intense part of the plasma emission, reducing noise from continuous plasma radiation or ambient light.
(4) Dust and Debris Mitigation: A vacuum system in the inspection container reduced the presence of dust and debris, which could obscure the laser-sample interaction or interfere with spectral readings.

A noteworthy aspect of the system's design is the ingenious incorporation of multiple reflective mirrors, which facilitates the simultaneous monitoring of RCA on two separate conveyor belts with the use of only one Nd:TAG laser. This innovative approach not only reduces the associated costs but also amplifies the system's overall operational efficacy.

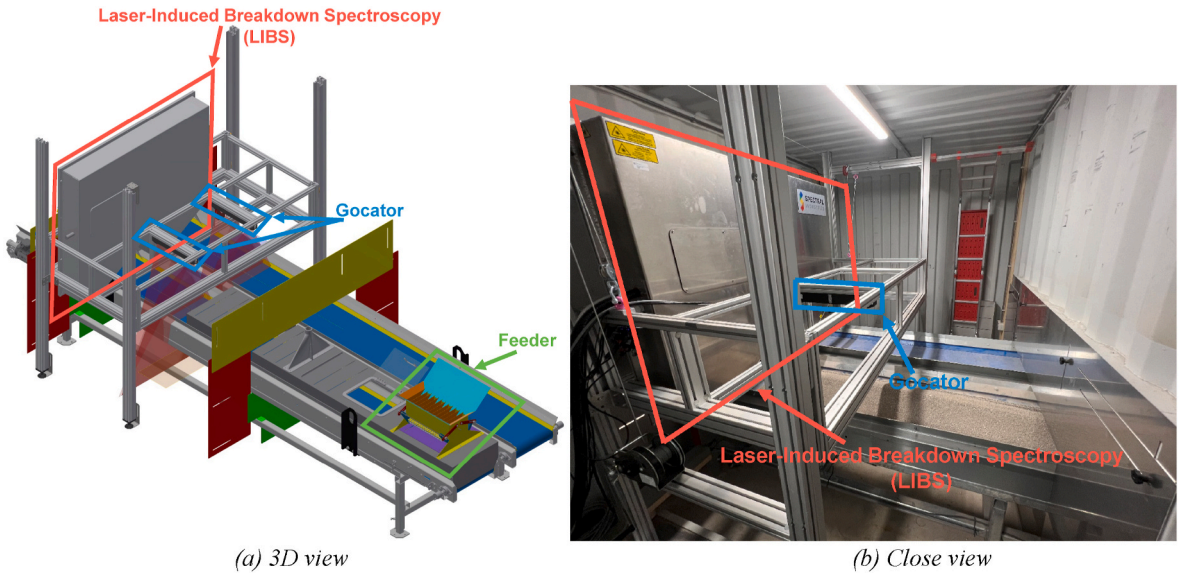

(a) 3D view (b) Close view

Fig. 4. Sensor-based quality inspection system.

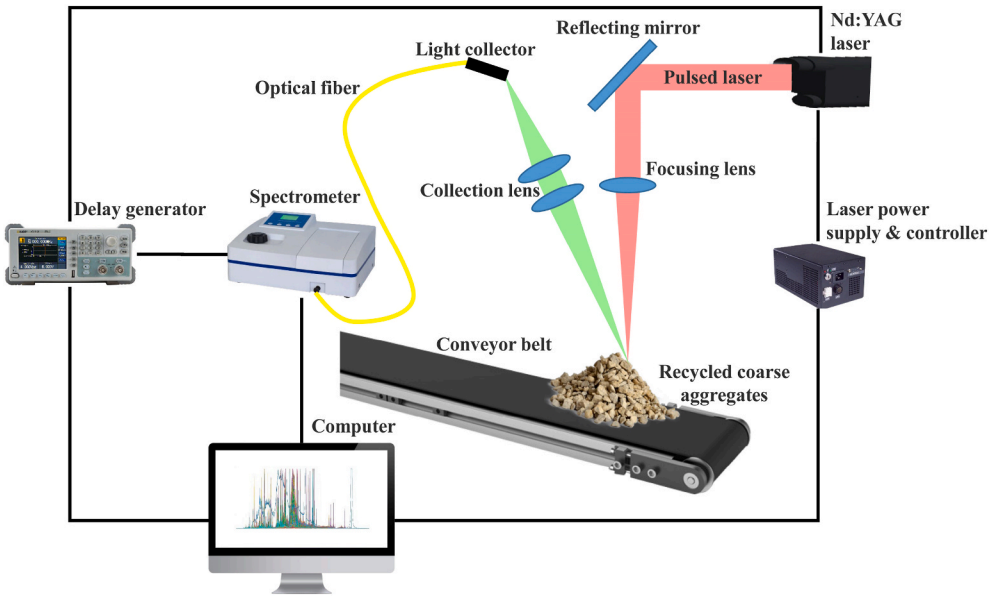

Fig. 5. Schematic diagram of LIBS.

Table 2
Experimental parameters.

Parameter	Value	Description
Laser Pulse Wavelength (nm)	1064	Nd:YAG laser, suitable for high-precision spectroscopic analysis.
Laser Pulse Frequency (Hz)	100	Balances high-resolution data acquisition with system throughput.
Laser Pulse Energy (mJ)	170	Generates plasma effectively while minimizing surface damage.
Laser Pulse Duration (ns)	6	Provides a concentrated energy burst for plasma generation.
Focal Length of Lens (mm)	300	Optimizes laser energy density for uniform plasma generation.
Conveyor Belt Speed (m/s)	0.529	Ensures uniform material inspection at high throughput.

2.2.3. Inspection

The inspection process begins with the introduction of RCA into the system via a feeder, followed by their deposition onto the conveyor belt, resulting in the formation of a triangular-shaped pile of RCA. This triangular configuration is designed to ensure a uniform distribution of the RCA, extending from the innermost region to the outer edges of the pile (Fig. 6). This deliberate arrangement is particularly advantageous as it optimally facilitates the surface inspection conducted by the Gocator, allowing for precise assessment and estimation of RCA properties.

As RCA piles move along the conveyor belt, they are sequentially inspected by both the Gocator and LIBS sensors. The data generated during these inspections are instantaneously recorded in a computer system and subsequently uploaded to a secure cloud storage platform for long-term archiving and retrieval. Additionally, monitoring data are also linked to radio frequency identification (RFID) tags attached to the piles to enhance traceability. The conveyor belt operates at a constant velocity of 0.529 m/s, enabling a single conveyor belt to transport more

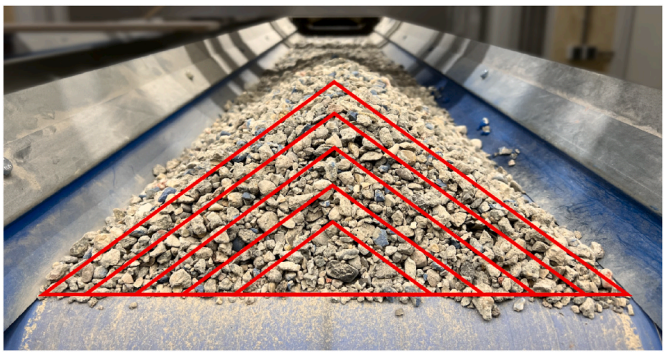

Fig. 6. Layered formation of RCA piles.

than 50 tons of RCA per hour.

2.3. Analysis methods

2.3.1. Particle morphology

The primary objective of the particle morphology analysis is to achieve a statistically representative and geometrically characterization of RCA particles, ensuring that the morphological features such as size, shape, and orientation are comprehensively and reliably captured. This characterization is crucial for understanding the behavior and performance of RCA in various applications, particularly where particle shape and distribution significantly impact material properties.

The feeding method for the RCA piles is meticulously designed to ensure symmetry, which justifies focusing the analysis on only one side of the piles. This symmetric feeding method guarantees that the particle distribution within the heap is uniform, allowing the segmentation and analysis process to be both efficient and representative of the entire pile.

Employing the Fastscape algorithm (Braun and Willett, 2013), originally developed for terrain analytics, the system performs a watershed segmentation process (Steer et al., 2022) of 3D point clouds to accurately delineate RCA particles. The segmented regions are then encapsulated within ellipsoidal envelopes, enabling a quantifiable analysis of particle morphology, structure, and orientation. This method addresses challenges such as over-segmentation and ensures accurate geometrical representation through ellipsoidal fitting, providing a comprehensive statistical and geometrical description of RCA particles. The process involves several steps:

Initial segmentation: The procedure begins by applying the watershed algorithm, traditionally used for 2D digital elevation models, to segment global 3D point cloud data. This adaptation allows the algorithm to effectively delineate individual particles by treating peaks in the data as watershed ridges, thereby dividing the data into distinct segments.

Segmentation correction: Commonly, the initial segmentation can result in over-segmentation, where particles are divided into smaller, unnecessary parts. To correct this, the method merges particles that are closely located. This merging is based on two criteria: the proximity of the particles' summits and the alignment of their surface normals. Additionally, particles that are excessively flat or elongated are removed. These steps refine the segmentation and enhance the overall quality.

3D ellipsoidal fitting: After the particles have been segmented and appropriately labeled, the next step is to characterize their geometrical properties. This is done by fitting 3D ellipsoids to each particle. Ellipsoidal fitting involves a complex optimization process where the best-fitting ellipsoid is calculated to approximate the shape and size of each particle. This step is crucial as it quantifies the particle structures, which can be vital for further analysis and applications.

Morphological Analysis: This method provides detailed geometrical information like the size, shape, and orientation of each particle. These properties are derived from the dimensions and orientation of the fitted ellipsoids. The key aspect of this ellipsoidal model is the choice of the second shortest axis as the main parameter for measuring graduation information. This particular axis is selected because it effectively represents the particle size, and consequently, helps in determining the PSD. The use of this axis is beneficial because it strikes a balance, being more informative than the shortest axis, which might be too small to provide useful data, and less variable than the longest axis, which could be too sensitive to minor changes in particle shape. This makes the second shortest axis a reliable and representative measure for assessing the characteristics of different particles in a sample.

2.3.2. 3D modeling with X-ray tomography

To further verify the accuracy of algorithms simulating particle morphology, medical imaging techniques are employed to scan samples of RCA piles. It is important to note that this imaging process is not part of the container technology but is instead used for offline verification and calibration purposes. This enabled the creation of 3D models of their interior to capture the actual particle morphology for comparison. Computed Tomography (CT) imaging, a commonly used modality (Basu et al., 2011), employs X-rays to acquire multiple angular projections of an object, which are then used to reconstruct the object's linear attenuation coefficient distribution. The resulting images are typically assembled into a series of consecutive axial slices arranged in parallel (Pelc, 2014). CT scan information is digitally archived, frequently in a format referred to as Digital Imaging and Communications in Medicine (DICOM). This format arranges the information into an organized collection that includes both the imaging data and related metadata (Fajar et al., 2022). Metadata parameters like slice thickness, instance number, pixel spacing, rescale slope, and rescale intercept found in DICOM files are employed during the data preprocessing phase.

The Hounsfield unit (HU) scale, employed in CT imaging, quantifies the radiodensity of tissues and materials. It sets the baseline with water at 0 HU and air at roughly −1000 HU, where substances of greater density show higher HU values. The process of converting the linear attenuation coefficient of each material at a specified effective energy into HU uses the standard equation:

$$\mathrm{HU} = \left(\frac{\mu_{\mathrm{material}} - \mu_{\mathrm{water}}}{\mu_{\mathrm{water}}}\right) \times 1000 \tag{1}$$

where μ represents the linear attenuation coefficient. In the process known as Hounsfield scaling or CT number scaling (Huda and Slone, 1996), raw attenuation values derived from CT scans are converted into Hounsfield units using the equation:

$$\mathrm{HU} = (\mathrm{PV} \times RS) + RI \tag{2}$$

where PV signifies the pixel value, representing the original value attributed to a pixel within a CT scan. *RS*, recognized as the rescale slope, is a scaling factor employed to modify the pixel values accordingly. Meanwhile, *RI*, identified as the rescale intercept, denotes a particular offset value applied to alter the pixel values.

Retrieving pixel arrays from DICOM files, organized by the instance number found in the metadata, involves adjusting each pixel's value in the CT image based on the rescale slope and intercept values. This process standardizes the pixel values to accurately represent the actual attenuation coefficients. Following this standardization, the pixel values are then transformed into HU.

To facilitate a comprehensive comparison with algorithms that simulate particle morphology, adopting a distinct methodology involving the CT scanning of samples becomes imperative. Conventional CT scanning techniques typically involve making equidistant vertical incisions through the sample to capture cross-sectional imagery. However, to enhance the comparability, it is crucial that slices are made at uniform intervals along an oblique plane parallel to the surface of the sample. This procedure demands the compilation of CT scan images into

a cohesive ensemble, which is then used to construct a 3D model of the sample, employing the transformed HU values. Subsequently, this model undergoes re-sectioning to align with the comparative analysis requirements.

2.3.3. Dice similarity coefficient

To assess the extent of overlap between results obtained from algorithmic simulations and X-ray tomography, the Dice similarity coefficient (DSC) is employed. The Dice coefficient is a statistical metric used to measure similarity, often applied in image processing to gauge spatial overlap. Its values range from 0 (indicating no overlap) to 1 (indicating perfect overlap). This measurement method provides a quantitative way to compare the accuracy and alignment of the two sets of data, facilitating an objective evaluation of how closely the simulation results mimic the X-ray tomography findings.

The Dice coefficient (Dice, 1945; Sørensen, 1948), also known as the Sørensen–Dice coefficient, is a statistical tool used to measure the similarity between two samples. In the context of image processing, the Dice coefficient is often used to quantify the spatial overlap between two images. The Dice coefficient is defined as:

$$DSC = \frac{2 \times |A \cap B|}{|A| + |B|} \tag{3}$$

where:

$|A \cap B|$ is the size of the intersection of two sets (in the context of images, these would be pixel sets) – basically, the number of pixels that are classified as the foreground (or as a particular object) in both images. $|A|$ is the number of pixels classified as the foreground in the first image. $|B|$ is the number of pixels classified as the foreground in the second image.

The value of the Dice coefficient ranges from 0 to 1, where 0 indicates no overlap and 1 indicates perfect overlap. This coefficient is particularly useful as it quantifies the similarity between two binary images. In an ideal case, if the predicted segmentation matches the ground truth segmentation exactly, the Dice coefficient would equal 1.

2.3.4. Contaminant detection

Contaminant detection in RCA is achieved by employing spectral analysis. This study builds upon the cluster-based identification algorithm (Chang et al., 2022), which improved data representation. The current research focuses on refining this algorithm to further increase its operational efficiency and adaptability. These refinements lead to more reliable contaminant identification by improving the accuracy and speed of the detection process. In the dynamic field of spectroscopic analysis, environmental factors influence LIBS spectra, making adaptability to new data crucial for maintaining model accuracy and relevance (T. Chen et al., 2020; Wang et al., 2021). Therefore, periodic calibration is necessary. The incremental learning technique provides a practical approach for real-time spectral data analysis. This method significantly enhances performance and flexibility by eliminating the need for complete model retraining, making it well-suited for applications in environments where data is continuously generated.

(1) Data preprocessing: To efficiently process spectral data, it is necessary to preprocess the raw data. Analysis has shown that focusing on the wavelength range of 200–900 nm is sufficient to achieve the desired outcomes, thereby improving computational efficiency. This preprocessing includes standardizing the spectral values to ensure uniform magnitude scales across different datasets, thereby highlighting unique data characteristics. Z-score standardization is used to maintain the data's distribution while aligning its mean and standard deviation to zero and one, respectively. This standardization captures essential data characteristics, such as the distribution patterns of peaks and troughs.

(2) Parallel processing for enhanced principal component analysis computations

Each laser pulse generates a spectrum denoted as $S = (s_1, s_2, \ldots, s_N)$, where s_i $(i = 1, 2, \ldots, N)$ represents the intensity of plasma emission at wavelengths λ_i. N is the total number of measured wavelengths. This method positions each laser pulse into an N-dimensional space, creating distinct clusters for different materials based on their spectral signatures. New laser pulses are either assimilated into existing clusters or identified as outliers based on how much their spectra deviate from the norm.

The axes of the coordinate system of S can be scaled and rotated to simplify the multi-dimensional normal distribution of points within a cluster. This simplification is achieved by defining a new orthonormal coordinate system, represented by N unit vectors $\alpha = (\alpha_1, \alpha_2, \ldots, \alpha_N)$. In this new coordinate system, the multi-dimensional normal distribution decomposes to N independent one-dimensional normal distributions, each aligned with a new axis. Thus, the spectrum in the database transforms into the new coordinate system as:

$$\xi = (\xi_1, \xi_2, \ldots, \xi_N) = (S \cdot \alpha_1, S \cdot \alpha_2, \ldots, S \cdot \alpha_N) \tag{4}$$

Effective categorization does not require all N dimensions; a smaller number n is sufficient. This reduction minimizes the influence of irrelevant or noisy parts of the emission spectra. The significant information is projected into the leading dimensions of the new coordinate system. After the principal component analysis (PCA) process, the spectral database for a cluster consists of the number n, the principal component vectors $(\xi_1, \xi_2, \ldots, \xi_n)$, and a center point $\bar{\xi}$ with variances σ^2, describing the multi-dimensional normal distribution of the spectra.

By leveraging optimized Basic Linear Algebra Subprograms (BLAS) and Linear Algebra PACKage (LAPACK) libraries and implementing parallel processing (Abdelfattah et al., 2021; Psarras et al., 2022), we can significantly enhance the efficiency of PCA computations. These improvements are crucial for handling large datasets, particularly in applications involving spectral data analysis, where computational demands are high.

The BLAS and LAPACK libraries are fundamental tools for performing efficient linear algebra computations (Frison et al., 2018; Psarras et al., 2022). BLAS provides low-level routines for common operations such as vector addition, scalar multiplication, dot products, and matrix multiplication. Optimized implementations, such as OpenBLAS and Intel Math Kernel Library (MKL) (Frison et al., 2020; Yamazaki et al., 2018), exploit modern CPU architectures to deliver significant performance improvements through multi-threading and vectorization. LAPACK extends BLAS functionalities by offering routines for more complex linear algebra problems, including solving linear systems, eigenvalue problems, and singular value decomposition (SVD). By leveraging optimized BLAS libraries, LAPACK routines can achieve high performance across various hardware architectures. Parallel computing libraries can parallelize independent tasks like computations on different data chunks. Optimized BLAS libraries internally use multi-threading for operations like matrix multiplication, which can be configured to utilize multiple threads.

(3) Cluster-based identification

Post-PCA, the database catalogs a material by assigning a finite number of principal components, n. This step defines a new coordinate system through n orthonormal vectors, facilitating the depiction of spectral data as multi-dimensional normal distributions around a centroid. Following normalization, principal component values are assumed to follow a chi-square distribution, which is crucial for classifying materials based on their spectral data. The conformity to the expected chi-square distribution is verified through P-value analysis, determining the significance level for recognizing specific materials.

Each component ξ_m $(m = 1, 2, \ldots, n)$ in the set $(\xi_1, \xi_2, \ldots, \xi_n)$ follows a normal distribution with a mean of $\overline{\xi_m}$ and a variance of σ_m^2. After applying z-score standardization, each standardized value Z_m is calculated as:

$$Z_m = \frac{\xi_m - \overline{\xi_m}}{\sqrt{\sigma_m^2}} \tag{5}$$

These standardized values follow a normal distribution with a mean of 0 and a variance of 1. To test if the data comes from a ${\chi_n}^2$-distribution, the chi-square value is calculated as:

$$\chi^2 = \sum_{m=1}^{n} {Z_m}^2 = \sum_{m=1}^{n} \frac{(\xi_m - \overline{\xi_m})^2}{\sigma_m^2} \tag{6}$$

This chi-square value helps determine the likelihood that the data follows the expected ${\chi_n}^2$-distribution. Each χ^2 can be converted into a probability *P*-value for the ${\chi_n}^2$-distribution. A higher χ^2 value corresponds to a lower *P*-value, indicating greater confidence that the data does not fit the expected distribution. *P*-values below a predetermined significance level indicate statistical significance. When this significance level is set as the acceptance criterion for a particular material, any spectra with *P*-value exceeding this threshold will be regarded as originating from that material.

(4) Incremental Learning

Implement incremental learning techniques to update the model as new spectral data becomes available. This can be achieved through online PCA methods and updating chi-square distribution parameters dynamically.

Given a new spectral observation S_t at time t (represents the index of the data point being introduced, i.e., it is the time step or the sequential position of the data point), the mean vector μ_t and covariance matrix C_t of the spectral data in the original *N*-dimensional space are updated using the following equations:

$$\mu_t = \mu_{t-1} + \frac{1}{t}(S_t - \mu_{t-1}) \tag{7}$$

$$C_t = C_{t-1} + \frac{1}{t}\left[(S_t - \mu_{t-1})(S_t - \mu_t)^T - C_{t-1}\right] \tag{8}$$

Here, the covariance matrix C_t is updated prior to performing PCA, capturing the variability of the spectral data in the original *N*-dimensional space. This updated covariance matrix reflects the latest statistical characteristics of the data, which is essential for accurately calculating the principal components. Subsequently, the principal components are extracted from the updated covariance matrix C_t using eigenvalue decomposition. In this approach, earlier spectral data are given the same weight as later spectral data, ensuring equal consideration throughout the time series. However, it is important to note that alternative methods exist, which prioritize more recent spectral data by assigning them higher weights, thereby adapting more swiftly to recent changes in the data.

Following PCA, the spectral data is transformed into a lower-dimensional space where each principal component follows a normal distribution. The chi-square distribution is then employed to evaluate the goodness-of-fit for new data points. To maintain the accuracy of this statistical test, it is essential to dynamically update the chi-square distribution parameters as new data is integrated.

Let ξ_t represent the vector of principal components at time t. The mean $\overline{\xi_t}$ and variance σ_t^2 of the principal components are updated incrementally:

$$\overline{\xi_t} = \overline{\xi_{t-1}} + \frac{1}{t}(\xi_t - \overline{\xi_{t-1}}) \tag{9}$$

$$\sigma_t^2 = \sigma_{t-1}^2 + \frac{1}{t}\left[(\xi_t - \overline{\xi_{t-1}})^2 - \sigma_{t-1}^2\right] \tag{10}$$

The chi-square statistic for the new observation ξ_t is computed as:

$$\chi_t^2 = \sum_{i=1}^{n} \frac{\left(\xi_{t,i} - \overline{\xi_{t,i}}\right)^2}{\sigma_{t,i}^2} \tag{11}$$

By continuously updating $\overline{\xi_t}$ and σ_t^2, the model dynamically adjusts to reflect the latest data distribution, thereby improving classification accuracy and robustness.

This method demonstrated a substantial reduction in computational load compared to traditional batch PCA, while maintaining similar levels of dimensionality reduction efficacy. Additionally, the dynamic updating of chi-square parameters facilitated more accurate and responsive classification, particularly as new data was introduced.

3. Results and discussion

3.1. PSD calculation

3.1.1. 3D point cloud data

Given the observed uniformity and consistency in the distribution pattern of constituents within the RCA piles, it becomes feasible to extrapolate the PSD characteristics of the entire pile through a focused analysis of the PSD associated exclusively with the outer surface layer of the pile. This method presents an effective means of obtaining a representative understanding of the overall PSD of the RCA piles. Using the Gocator scanner, a comprehensive scan of the RCA pile's external surface was conducted, yielding detailed 3D point cloud data (Fig. 7 (a)).

The spatial resolution of this 3D point cloud data is crucial as it affects the accuracy and detail of the RCA particle measurements. In this context, it's paramount to note that the resolution of the point clouds under study demonstrated discernible variances across different spatial orientations—a phenomenon that has broader implications for the precision of granulometric assessments.

In the direction parallel to the motion of the conveyor belt, the resolution of 3D point cloud data is influenced by two factors. The first factor is the velocity of the conveyor belt, controlled by adjusting the rotational speed of the motor drive. This rotational speed adjustment is achieved through the manipulation of the motor's output frequency and the number of poles. Specifically, the motor drive in this study operates at 50 Hz with a 4-pole design, resulting in a rotational speed of 1500 rpm. Mechanical adjustments include a gearbox ratio of 19 and a wheel perimeter of 401.92 mm, resulting in a conveyor belt speed of 0.529 m/s. The second factor affecting the resolution is the encoder resolution of the Gocator, which was calibrated to record 1024 ticks per revolution, translating to a point cloud resolution of 0.3925 mm along the conveyor belt's path.

Perpendicular to the conveyor belt, across its width, the resolution varies between 0.375 mm and 1.1 mm. This range is inherently tied to the Gocator's field of view at any given point in time. For accuracy, the transverse resolution was standardized at 0.375 mm in this study.

Vertically, concerning the height or depth of the RCA piles, the Gocator's advanced internal mechanisms come into play. The system provides a resolution gradient from a fine 0.092 mm to a coarser 0.488 mm. This variability highlights the scanner's versatility and adaptability in handling different granulometric scenarios, establishing it as a crucial tool in the comprehensive evaluation of RCA piles. In this study, the resolution was set at 0.092 mm in the vertical dimension.

3.1.2. PSD calculation

The PSD of RCA piles was determined using the method described previously. This involved fitting the 3D point cloud data of the RCA piles into ellipsoidal models (Fig. 7 (b)) to capture morphological data for each particle. The resulting PSD was effectively demonstrated through a

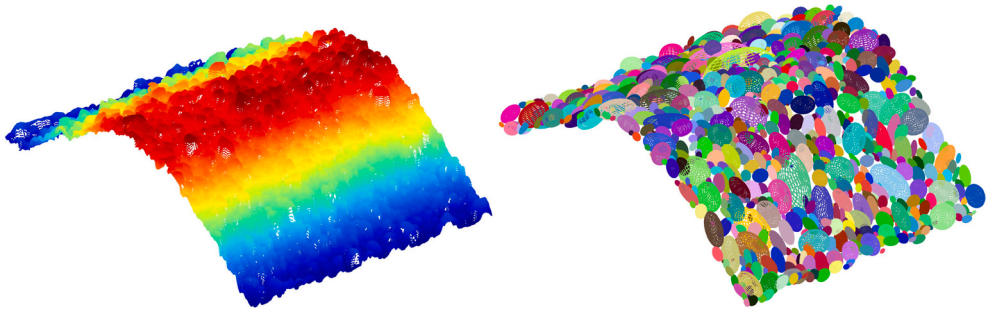

(a) 3D view of the point cloud data (b) Ellipsoids fitted to each particle

Fig. 7. Point cloud processing.

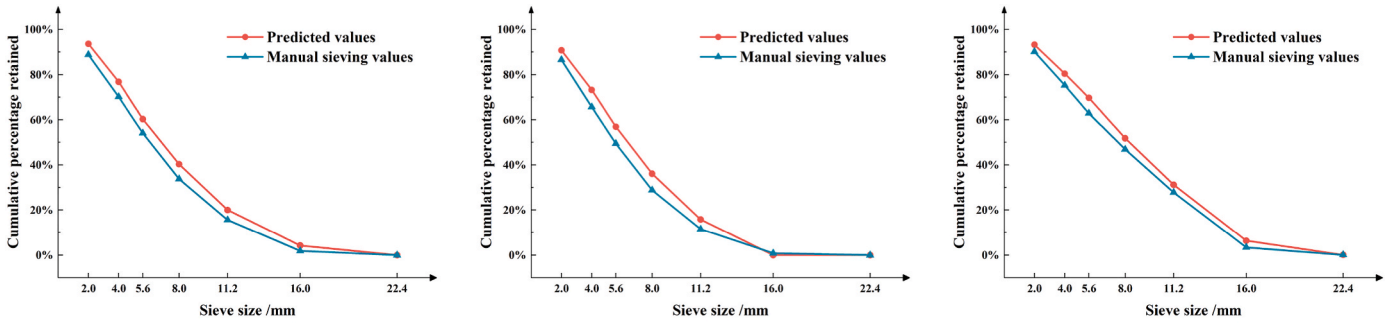

(a) Test 1 (b) Test 2 (c) Test 3

Fig. 8. Cumulative percentage retained graphs.

cumulative percentage retained graph, as depicted in Fig. 8. This graph, supported by calculations of ellipsoidal volume and the RCA's apparent density, provided a clear visualization of the PSD characteristics inherent to the RCA piles. The insights gained from this analysis are crucial for understanding the aggregate structure and its potential influence on the performance of concrete.

Subsequently, a cross-referential analysis was conducted to validate the accuracy and reliability of this non-intrusive, surface-based technique for PSD determination. This entailed comparing the PSD results from the 3D point cloud data with those obtained through the traditional, more invasive method - manual sieving. The comparison aimed to ascertain the degree of correlation and consistency between the surface PSD measurements and the actual overall PSD of the entire RCA piles. Fig. 8 depicts this comparative study, showing the cumulative percentage retained curves as predicted from 3D point cloud analytics against those obtained from manual sieving, based on pilot scanning trials. The results indicate a minimal difference between the two methods, affirming a high degree of accuracy in the surface-based technique.

To further assess the precision and efficacy of this surface-based PSD measurement technique, the Root Mean Square Error was calculated between the predicted and manually derived values, resulting in deviations of 4.93%, 5.38%, and 4.27% across three experiments. These low Root Mean Square Error values confirm the robustness and precision of this surface-based technique in estimating the PSD of RCA piles on a conveyor belt. Initial results demonstrate a high degree of concordance between the two methods, suggesting that the 3D scanning approach could effectively approximate the comprehensive PSD with a significant reduction in manual effort and time.

3.1.3. X-ray tomography validation

To further validate this surface-based PSD measurement technique,

(a) Sample box (b) Processed 3D scanning model (c) Processed X-ray tomography model

Fig. 9. RCA sample.

X-ray tomography was employed to capture the morphology of particles beneath the surface of RCA plies. The internal structure captured by X-ray tomography was compared to the ellipsoids simulated from 3D point cloud data. A black box (as shown in Fig. 9 (a)) was used to simulate the inclined surface on one side of the formed piles, with RCA spread inside. The sample was scanned using both 3D scanning and X-ray tomography techniques. The data processed from these methods are shown in Fig. 9 (b) and (c) respectively.

The ellipsoidal fitting model illustrated in Fig. 9 (b) originated from 3D point cloud data obtained through 3D scanning with the Gocator. This process involved segmenting the 3D point cloud data and fitting it to the ellipsoidal shape. The 3D model in Fig. 9 (c) was generated through layered scanning with X-ray tomography. This process involved compiling each scanned layer and isolating the particle components using thresholding. Both models were incrementally sliced from top to bottom, parallel to the inclined surface, allowing observation of each layer's cross-section. Then the two obtained cross-sectional images of each layer were overlapped for comparative analysis. Six representative layers were selected in Fig. 10, following the top-down slicing depth. On the left are the cross-sectional details of the simulated ellipsoidal model. In the middle are the cross-sectional details derived from the 3D model constructed using X-ray tomography, reflecting the real particle distribution. On the right are the overlapping cross-sections of the two cutting methods for comparison.

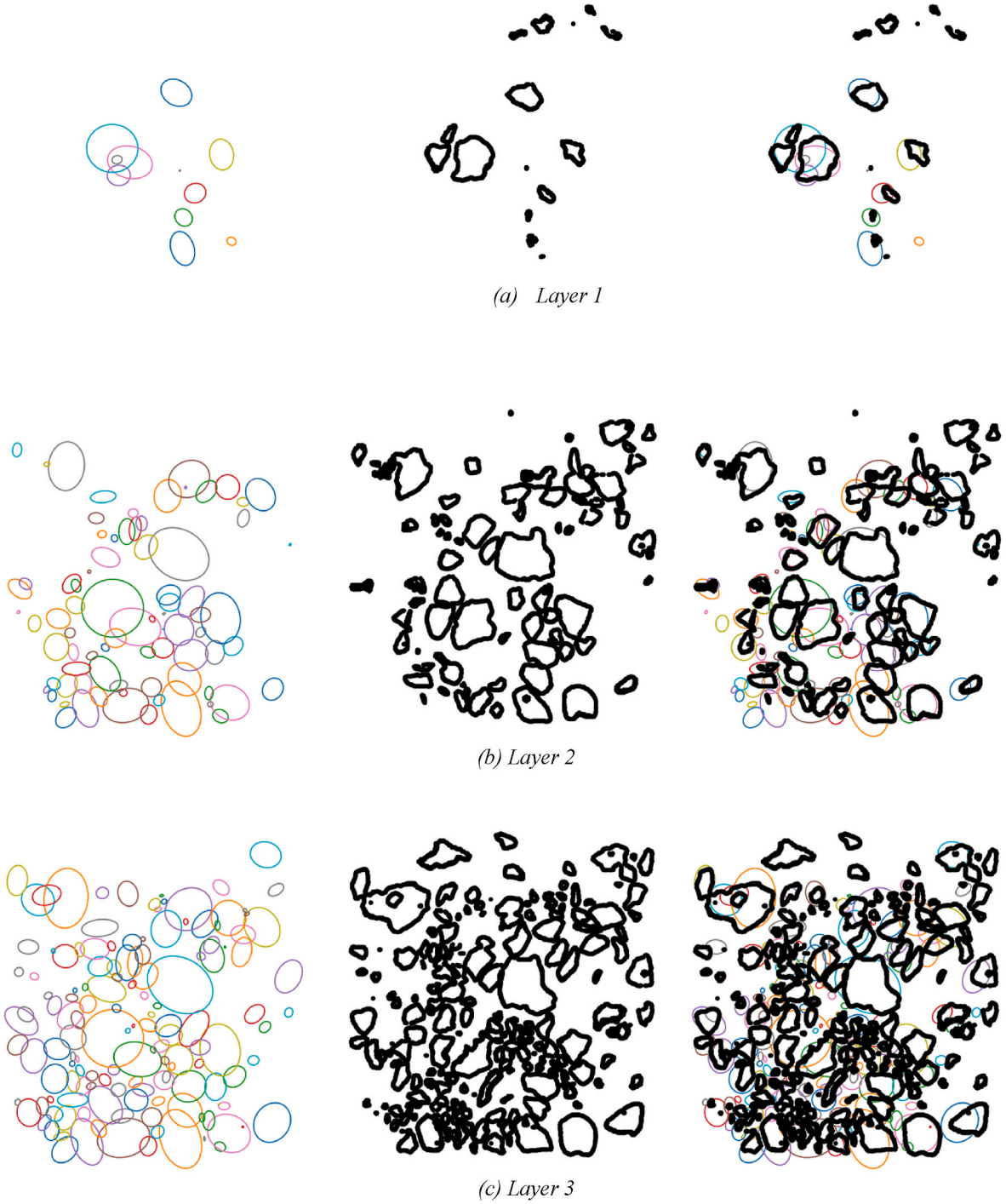

Fig. 10. Cross-sectional details.

(d) Layer 4

(e) Layer 5

(f) Layer 6

Fig. 10. (*continued*).

To assess the similarity between cross-sections obtained by the two methods, the DSC was employed. Following the sequence depicted in Fig. 10, from (a)–(f), the DSC values are 0.63, 0.71, 0.82, 0.85, 0.86, and 0.82. From the selected sections, an incremental increase in overlap between the two methods is evident, peaking at 0.86 before slightly decreasing. Initially, lower overlap occurs due to irregularities on the particle surfaces, challenging their representation in the simulated ellipsoids. As the sections progress, the ellipsoids better emulate the internal particle distribution, maintaining an overlap of around 0.8. However, in deeper sections of the ellipsoids, a gradual appearance of blank spaces in the lower-left region is observed. This is attributed to the presence of numerous smaller particles in that area. 3D scanning only captures information from the top layer, hence forming a single layer of smaller ellipsoids. In contrast, X-ray tomography does not encounter this limitation, as additional particles fill the same location, preventing the appearance of blanks.

This comparative analysis further validates the reliability of surface-based PSD measurement techniques. Consequently, the Gocator 3D scanning can be employed for a quick and convenient estimation of PSD.

3.2. Contaminant detection

This study aimed to evaluate the performance differences of the LIBS sensor in capturing spectra from objects under varying environmental conditions. The focus was on assessing its ability to adapt to new data to maintain model accuracy and relevance in dynamic spectroscopic analysis. Additionally, the study aimed to understand how the movement of the conveyor belt might affect the effectiveness of the system's reflective mirrors. Spectral measurements from a wide range of materials were recorded under two conditions: while the conveyor belt was running and while it was stationary.

Fig. 11 provides a visual representation of the findings. The results reveal minimal variation in the spectra from the materials, regardless of the conveyor belt's motion. The minor differences in spectra observed between the moving and stationary states of the conveyor belt do not significantly impact the overall system performance. This uniformity

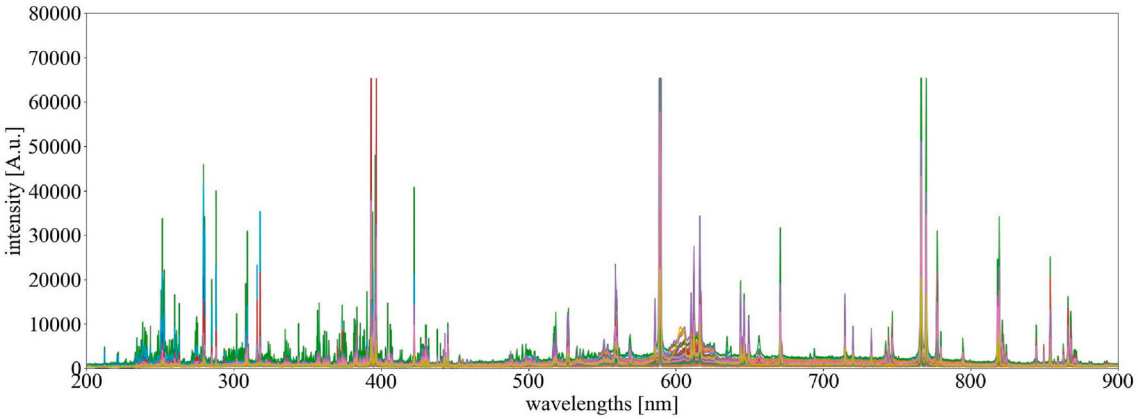

(i) Conveyor belt in the operational state

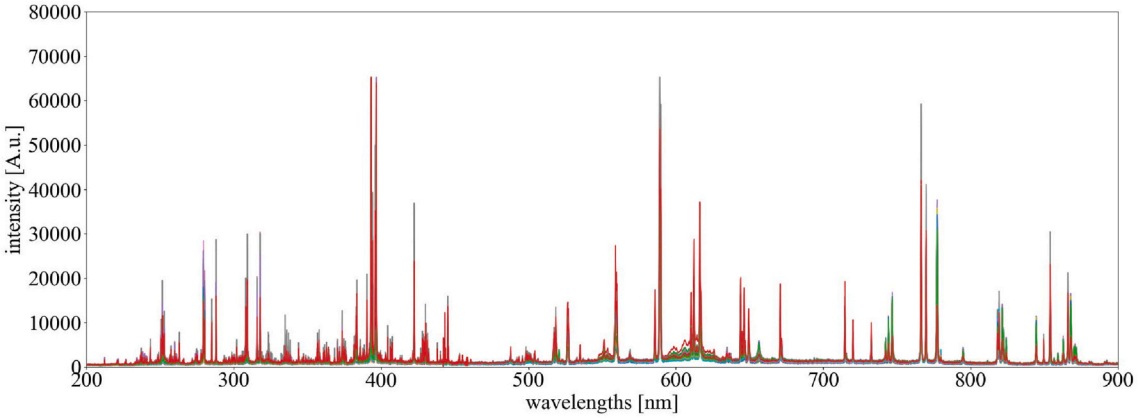

(ii) Conveyor belt in the stationary state
(a) Brick

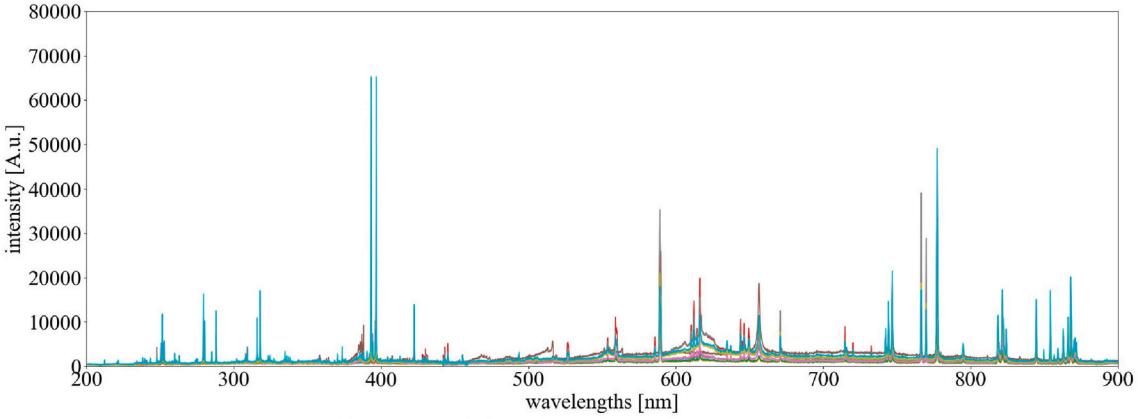

(i) Conveyor belt in the operational state

Fig. 11. Comparison of spectra of different materials in the operation and stationary states of the conveyor belt.

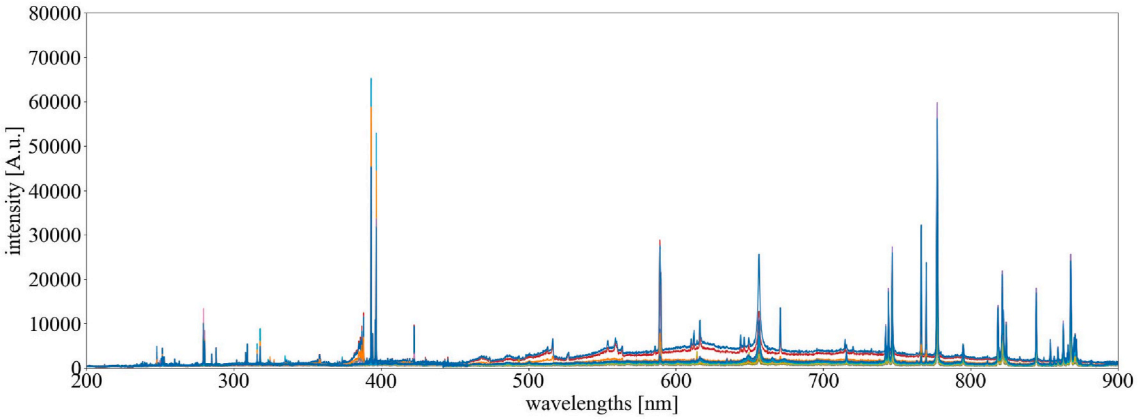

(ii) Conveyor belt in the stationary state
(b) Foam

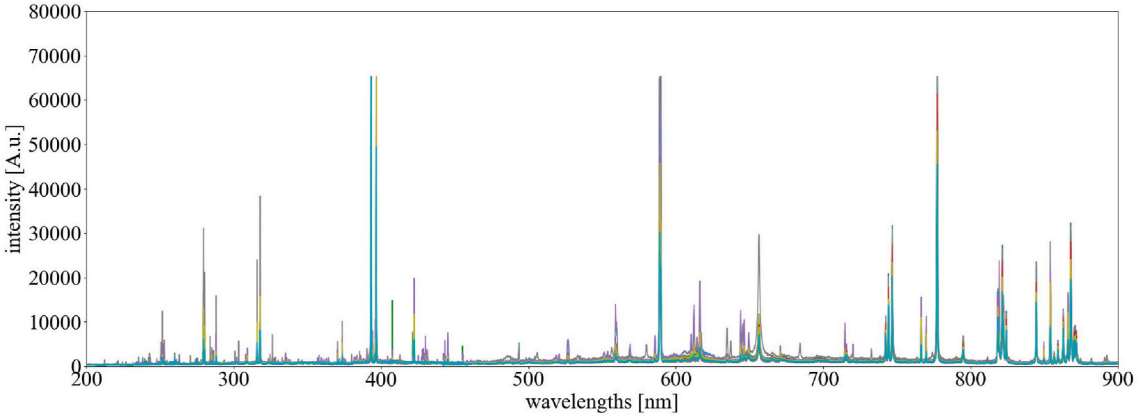

(i) Conveyor belt in the operational state

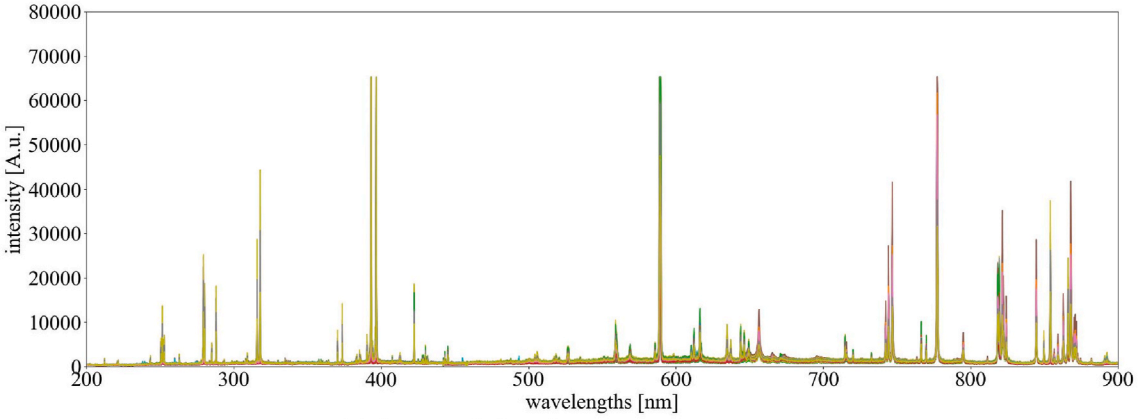

(ii) Conveyor belt in the stationary state
(c) Glass

Fig. 11. (*continued*).

demonstrates the reliability and effectiveness of the system's design. It also supports the system's ability to perform consistently under different operational scenarios. Its resilience under different operational conditions underscores its potential as a reliable tool for real-time industrial applications, ensuring consistent and accurate data acquisition regardless of conveyor belt activity. This is paramount for industries where conveyor belt speeds might vary, and where maintaining measurement consistency is critical.

Despite the general consistency, there were slight spectral differences noted between the moving and stationary states of the conveyor belt. These differences, though minor, could lead to errors when classifying materials with similar chemical compositions, such as recycled cement paste powder (RCP), recycled fine aggregates (RFA), RCA, and others. These subtle variations, although not significantly affecting

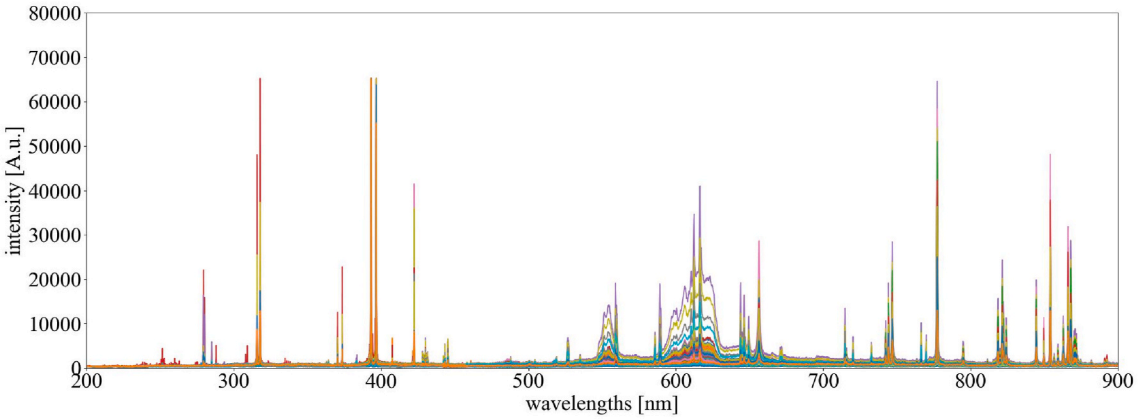

(i) Conveyor belt in the operational state

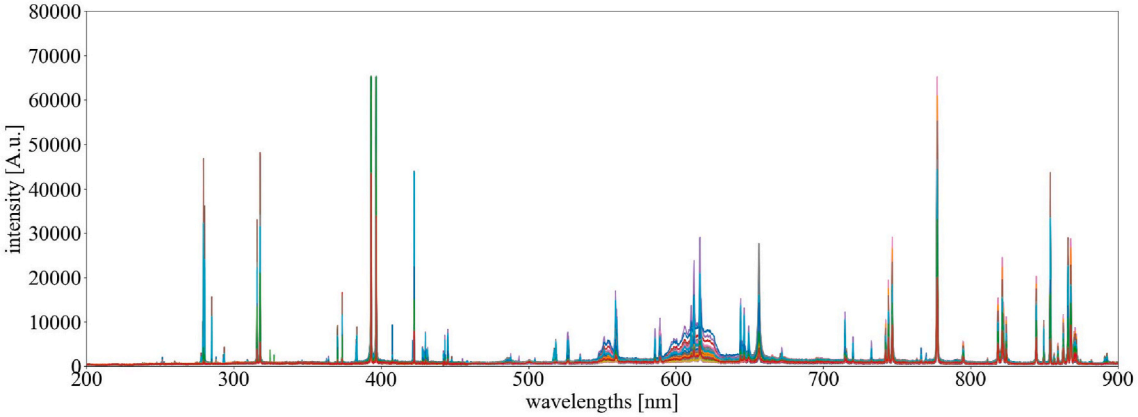

(ii) Conveyor belt in the stationary state
(d) Gypsum

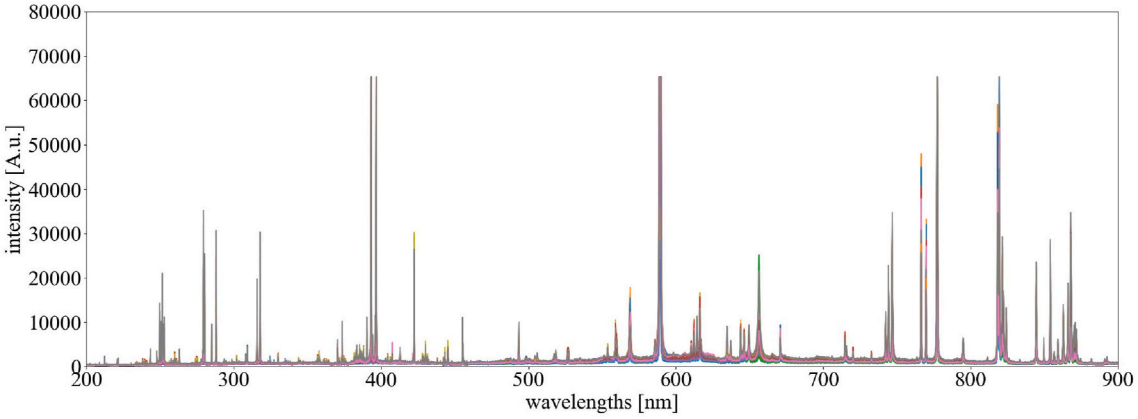

(i) Conveyor belt in the operational state

Fig. 11. (*continued*).

overall system performance, must be considered in detailed analyses to avoid misclassification and ensure accurate results.

After acquiring spectra from various materials, a systematic classification was conducted using a cluster-based identification algorithm enhanced by incremental learning techniques. This algorithm, recognized for its ability to group data by identifying inherent similarities, was applied to discern patterns within the updated spectral data. The model's performance underwent a thorough assessment to ensure its reliability for practical applications. Remarkably, the model showcased robust performance metrics for this new system: achieving an accuracy rate of 0.94, a weighted average precision of 0.95, a weighted average recall of 0.94, and an F1-score (weighted average) standing at 0.95 on the validation dataset.

These performance metrics confirm the effectiveness of LIBS as an analytical tool, especially for analyzing recycled concrete aggregates within industrial contexts. These metrics highlight LIBS's ability to deliver both accuracy and precision quickly, without compromising the quality of the outcomes. By adopting these advanced analytical

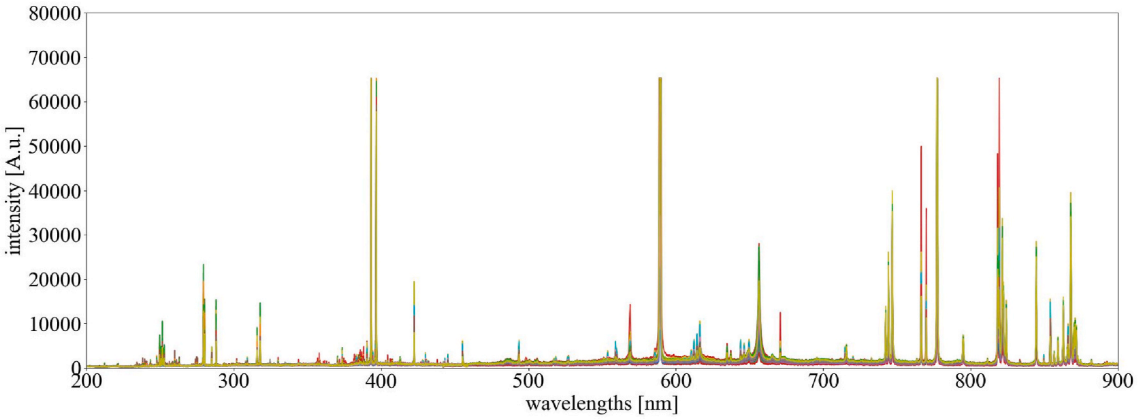

(ii) Conveyor belt in the stationary state
(e) Mineral fibers

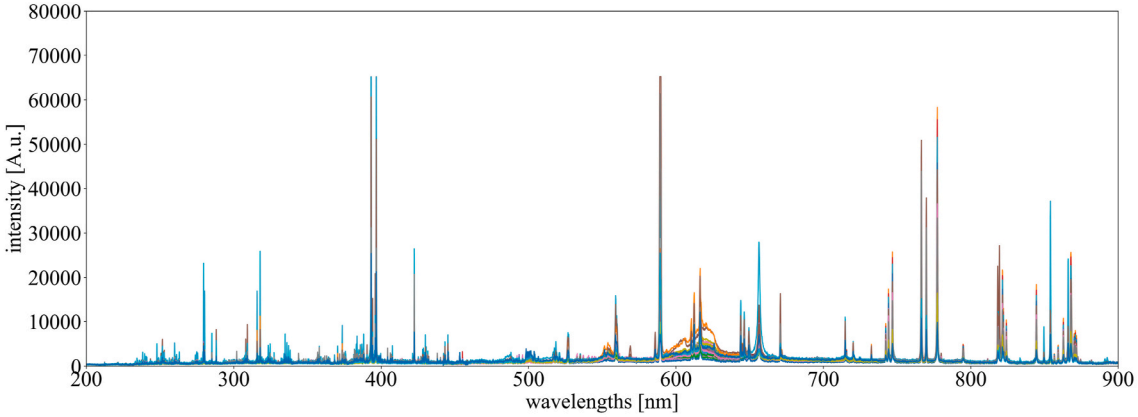

(i) Conveyor belt in the operational state

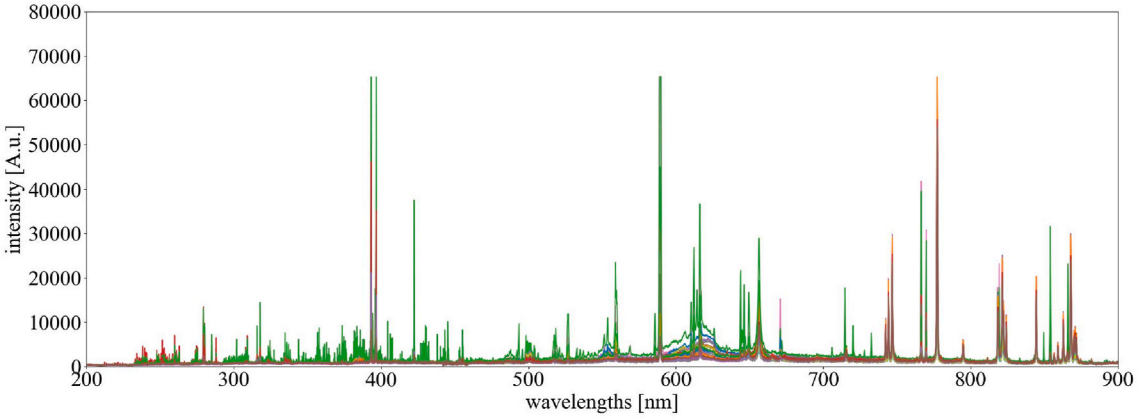

(ii) Conveyor belt in the stationary state
(f) Plastics

Fig. 11. (*continued*).

techniques, industries can confidently make strides forward, optimizing the use of recycled materials and maintaining high-quality standards.

3.3. Discussion on experimental conditions and limitations

While the proposed sensor-based quality inspection system demonstrates significant advancements in RCA quality assurance, several experimental variables require closer examination to assess their influence on system stability and accuracy. This section delves into key factors such as conveyor speed, sensor resolution, and environmental conditions, providing insights into the system's robustness and adaptability.

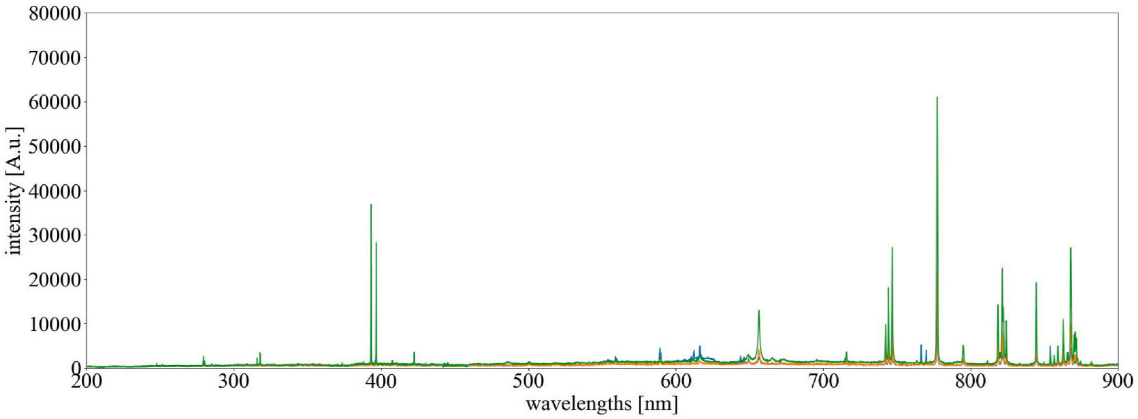

(i) Conveyor belt in the operational state

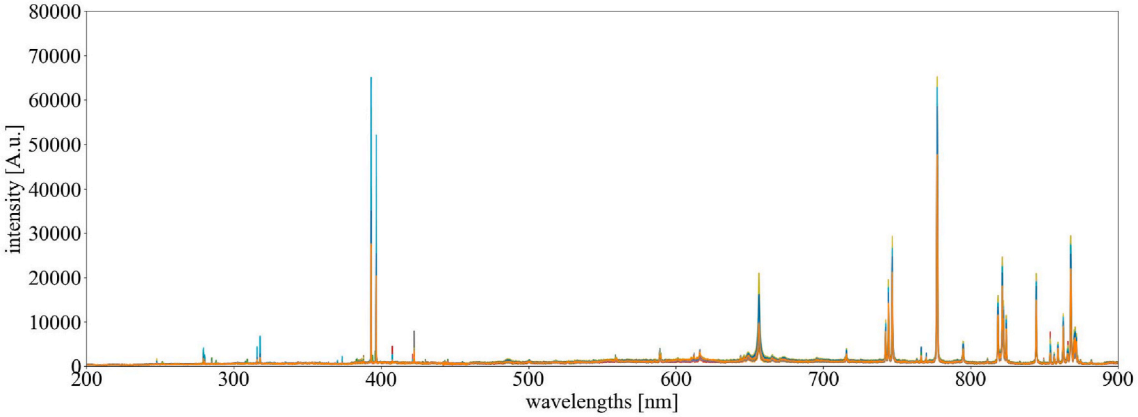

(ii) Conveyor belt in the stationary state
(g) Wood

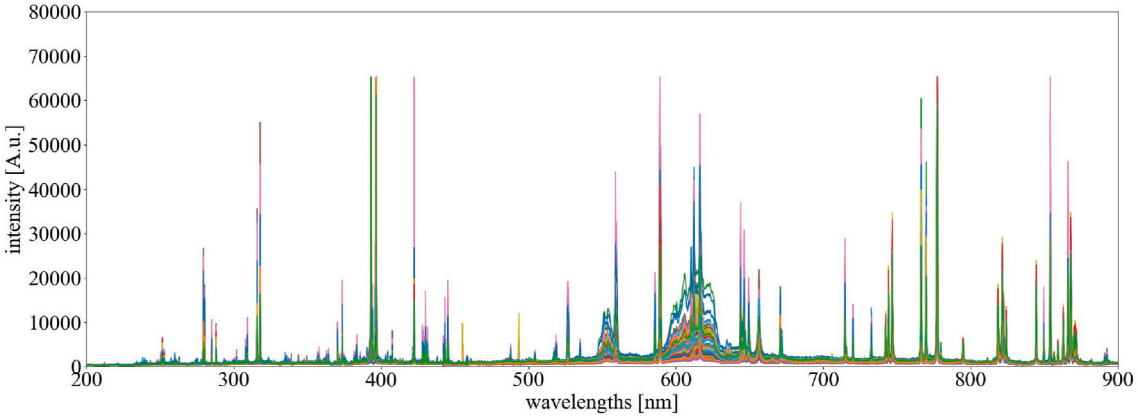

(i) Conveyor belt in the operational state

Fig. 11. (*continued*).

3.3.1. Conveyor speed

The conveyor belt speed was maintained at a constant velocity of 0.529 m/s during all experiments. This speed was chosen based on an optimization process that balances throughput and inspection accuracy. However, it is crucial to consider how variations in conveyor speed may affect sensor performance. At higher speeds, potential challenges include reduced time for laser-sample interactions in the LIBS sensor and lower resolution of 3D point cloud data from the Gocator scanner. Conversely, slower speeds could increase inspection time but improve data fidelity. Future studies should examine the trade-offs associated with different speeds, particularly in dynamic industrial settings where operational throughput requirements vary.

3.3.2. Sensor resolution

The spatial resolution of the 3D point cloud data varied depending on the orientation relative to the conveyor belt. Horizontal resolution ranged from 0.375 mm to 1.1 mm, while vertical resolution was set at 0.092 mm. These settings ensured detailed granulometric analysis but

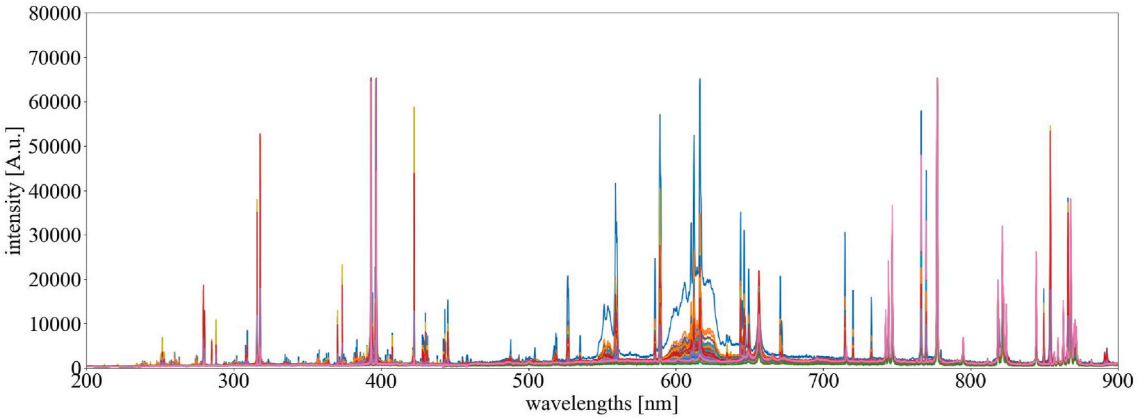

(ii) Conveyor belt in the stationary state
(h) Recycled cement paste powder (RCP)

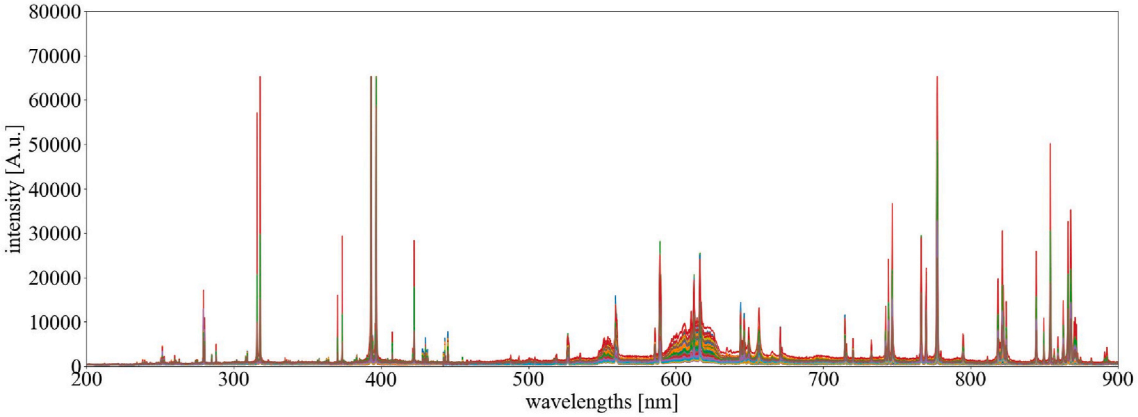

(i) Conveyor belt in the operational state

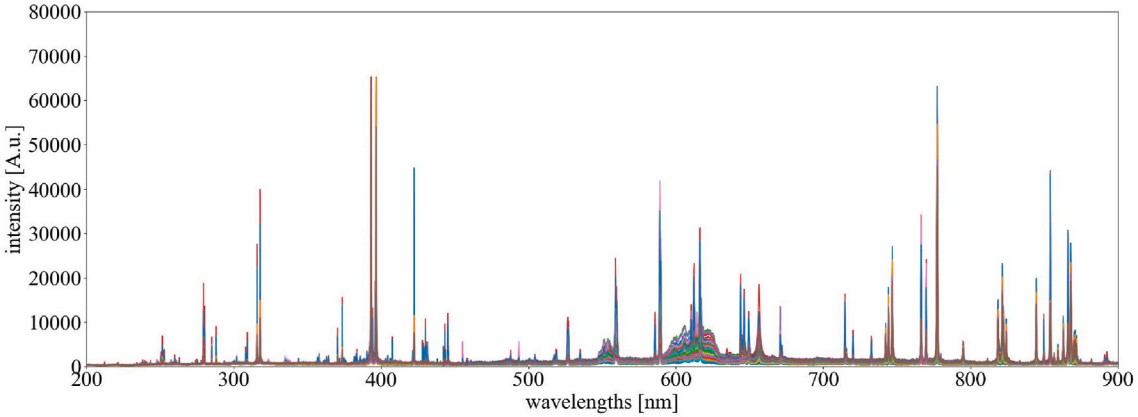

(ii) Conveyor belt in the stationary state
(i) Recycled fine aggregates (RFA)

Fig. 11. (*continued*).

may not account for scenarios involving smaller particles or high-density piles. Additionally, the LIBS sensor's temporal gating technique effectively mitigated noise but required precise synchronization to achieve optimal spectral acquisition. Investigating how resolution changes impact data accuracy under different particle size distributions and pile configurations is essential for refining system performance.

3.3.3. Environmental conditions

Environmental factors such as dust, lighting, and temperature fluctuations were controlled during experiments through the use of a vacuum system and an enclosed container. While these measures ensured accurate sensor readings, real-world conditions at demolition sites may pose additional challenges. To provide a comprehensive understanding of the sensor-based quality inspection system's performance in practical

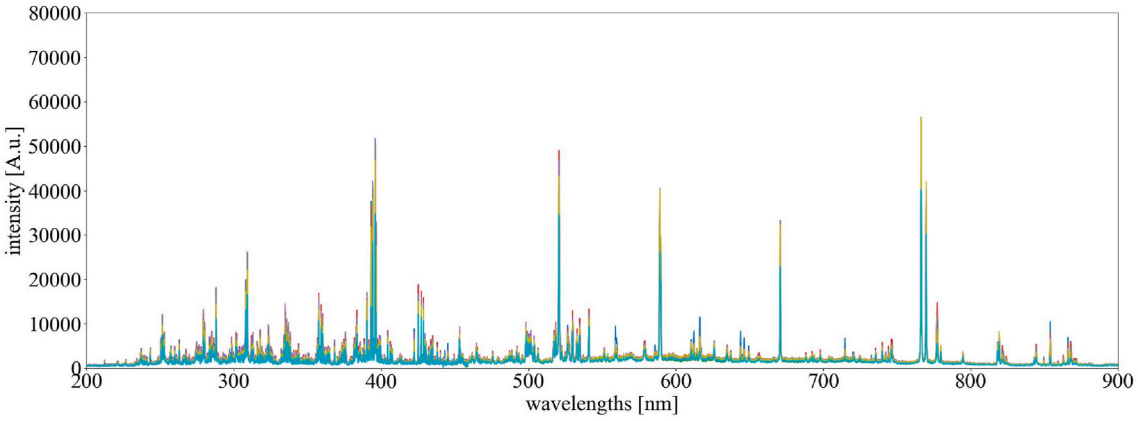

(i) Conveyor belt in the operational state

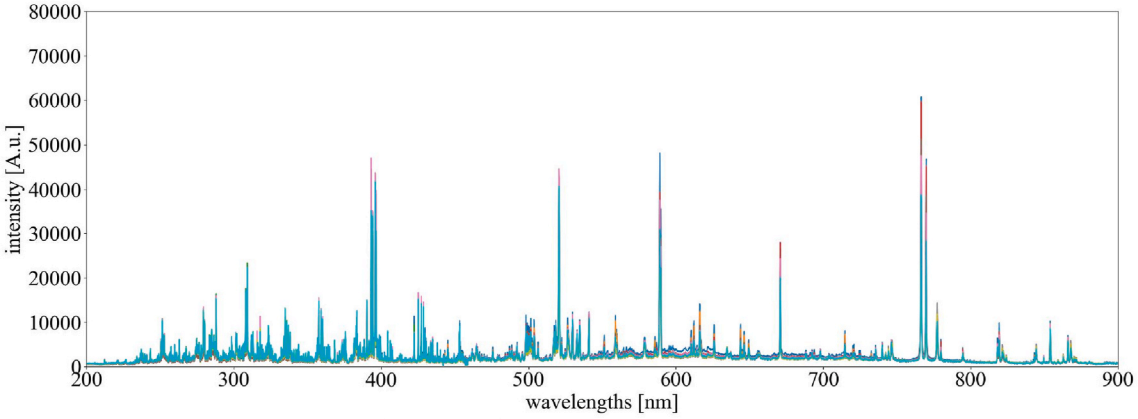

(ii) Conveyor belt in the stationary state

(j) RCA

Fig. 11. (*continued*).

scenarios, the following environmental factors and mitigation strategies are discussed:

(1) Dust and debris interference

Impact: High levels of dust and debris, common in demolition sites, can obscure the laser-sample interaction, reducing the accuracy of both 3D scanning and LIBS measurements.

Mitigation: The system employs a vacuum-based dust suppression mechanism, which enhances visibility and minimizes interference during data acquisition. Experimental results confirm a significant improvement in measurement consistency when dust levels are reduced. Future designs could integrate advanced filtration systems to further mitigate this challenge.

(2) Ambient lighting variations

Impact: Changes in ambient lighting, especially in outdoor applications, could potentially affect the optical components of the Gocator and LIBS systems.

Mitigation: The use of enclosed, containerized setups effectively shields the sensors from direct sunlight or variable lighting conditions. However, integrating adaptive calibration algorithms that adjust for residual lighting variability can further enhance robustness.

(3) Temperature fluctuations

Impact: Extreme temperature variations may influence the alignment of optical components or the performance of electronic systems, potentially leading to calibration drift.

Mitigation: Laboratory tests indicate that the system maintains stable performance within a broad operational temperature range. Incorporating temperature-compensating sensors or materials can enhance resilience in extreme climates.

(4) Material surface moisture

Impact: Surface moisture on RCA particles can alter the spectral response captured by LIBS, potentially leading to the misclassification of contaminants.

Mitigation: Pre-drying mechanisms or spectral correction algorithms can be introduced to account for moisture-induced spectral variations, ensuring more accurate material classification.

(5) Vibrations and conveyor belt motion

Impact: Vibrations from on-site machinery or inconsistencies in conveyor belt motion may affect the stability of sensor readings, especially during LIBS operations.

Mitigation: The use of time-resolved spectral acquisition and synchronization with belt movement ensures minimal signal distortion. Additional mechanical stabilizers could further reduce the impact of vibration-induced inaccuracies.

Understanding and mitigating these environmental factors are critical for deploying the system in diverse operational scenarios. While initial validations demonstrate the system's robustness, field trials in

harsher environments could provide further insights into its adaptability. By integrating advanced calibration techniques and environmental compensation mechanisms, the system's accuracy and reliability can be sustained across varied conditions.

3.3.4. Scenario variations and system adaptability

To evaluate the robustness of the system, further testing under diverse scenarios is recommended. For instance:

(1) Material Heterogeneity: The presence of varied contaminants, such as metals or polymers, may influence LIBS classification accuracy, especially for materials with overlapping spectral signatures.
(2) Pile Formation: The triangular configuration of RCA piles ensures uniform inspection but may not represent alternative deposition methods. Analyzing different pile geometries would help assess system scalability.
(3) Operational Scale: Scaling up the system to higher throughput levels or multiple conveyor belts might reveal bottlenecks in data processing or sensor synchronization.

The current study does not extensively quantify the effect of these variables across all possible operational conditions. While preliminary results suggest robustness in controlled environments, real-world applications may reveal additional constraints. Future work should incorporate advanced modeling and simulation techniques to predict performance under varying conditions. Additionally, integrating adaptive algorithms to adjust sensor parameters dynamically could further enhance system reliability in fluctuating environments.

4. Comparison to contemporary work

4.1. PSD analysis

Several recent studies (Bai et al., 2021; Fu and Aldrich, 2023; Hamzeloo et al., 2014; Z. Zhang et al., 2020) have primarily focused on using 2D image analysis for particle size detection in materials such as copper ore, coal, and rock. However, there is limited research specifically targeting particle size detection for RCA. In these studies, materials are typically spread flat on a conveyor belt, and in some cases, the particles do not overlap. This arrangement results from the inherent limitation of conveyor belt systems, which expose only one side of the material. Moreover, these methods are rarely scaled for on-site, high--throughput applications, leading to inefficiencies in industrial contexts. Additionally, most studies emphasize PSD of surface-level particles while neglecting the distribution of entire particle batches. Lu et al. (2024) proposed an improved lightweight rock object detection method using sieve sizes ranging from 20 mm to 200 mm for particle size studies. While this method improves upon approaches, it struggles with smaller particles. Particles near or below 20 mm are often unclear in the images, resulting in a relative measurement error of up to 14.13%. Moreover, the distribution of the finer fractions is estimated using fitting models rather than directly measured. This limitation is particularly significant for RCA, where particle sizes typically range from 2.0 mm to 22.4 mm—a size range inadequately addressed by current techniques.

To address these limitations, our system collects representative data to achieve integrating portability, high throughput, and precise PSD evaluation, making it suitable for industrial deployment. The system processes over 50 tons of RCA per hour on a single conveyor belt, marking a substantial improvement over laboratory-based methods, which are inherently constrained in scalability. Additionally, the results can be immediately uploaded to cloud systems for further processing and traceability, facilitating faster decision-making and improved quality control.

4.2. Contaminant detection

In the field of contaminant detection using sensors for industrial applications, most studies have concentrated on identifying contaminants in images through visual sensors. However, few have specifically addressed the challenges of detecting contaminants in RCA under real-world industrial conditions. For instance, Bobulski and Kubanek (Bobulski and Kubanek, 2021) employed a conveyor belt system integrated with a microcomputer for image processing to classify plastic waste into four categories, achieving an accuracy of 74%. Lohumi et al. (2021) developed an online inspection system using fluorescence and color imaging to detect foreign materials unintentionally introduced into fresh-cut vegetables. Nevertheless, their method failed to identify contaminants such as transparent low-density polyethylene, Styrofoam, small stepper pins, and needles. Mewada et al. (2024) applied advanced computer vision models for contamination detection in densely cluttered waste environments. The YOLOv8-x model achieved a mean average precision of 0.463 with the aid of transfer learning.

Compared to other sensors, the LIBS sensor offers significant advantages, including versatility, multi-element detection, and suitability for field applications (Brunnbauer et al., 2023). The LIBS sensor is commonly used for real-time detection of rapid changes in material composition, especially in the metalworking industry, where it aids in the classification of steel, various alloys, slag, and metal scrap (X. Chen et al., 2024; H. Kim et al., 2021; Park et al., 2021). While LIBS sensor excels in identifying components within a single material type, its application for real-time detecting diverse substances remains limited. Furthermore, its use in industrial settings for rapid contaminant detection in RCA on conveyor belts is rare. For example, Huber et al. (2014) demonstrated the use of the LIBS sensor for quasi-real-time identification of chlorine-containing waste polymers in an industrial sorting plant. This system enabled sorting based on chlorine concentration, particularly for polyvinyl chloride. Merk et al. (2015) developed a LIBS-based system for metal scrap identification directly on a conveyor belt. Similarly, Werheit et al. (2011)described the use of the LIBS sensor to identify aluminum alloys in post-consumer scrap during conveyor motion.

Despite these advances, implementing effective algorithms to process the spectra captured by the LIBS sensor is critical to ensure robust performance in dynamic industrial environments. Arbitrary sample shapes, surface contamination, and movement increase signal fluctuations compared to static conditions. Additionally, uncontrollable factors, such as environmental variability, can lead to data sparsity, adversely affecting classification model performance.

Our system achieves comparable accuracy to existing methods while excelling in adaptability. The LIBS sensor's ability to analyze materials in real time under dynamic conditions offers a significant advantage for industrial applications. Unlike many systems that require stationary samples for precise detection, the proposed system maintains consistent performance during conveyor belt motion. Spectral measurements reveal negligible variations between stationary and moving states, confirming its robustness. The incorporation of an incremental learning algorithm enables continuous adaptation to new spectral data without the need for retraining from scratch. Compared to other spectroscopic systems, this feature is particularly advantageous in environments with diverse contaminants and evolving material compositions.

5. Limitations and future orientations

5.1. Limitations

While the proposed sensor-based quality inspection system demonstrates substantial advancements in the processing and evaluation of RCA, it is not without limitations. These include:

(1) Operational Constraints: The system's performance was evaluated under controlled demolition site conditions. Variability in environmental conditions such as extreme weather, dust, and unexpected debris might impact system accuracy and reliability.
(2) Contaminant Spectrum: Although the LIBS sensor accurately identifies a wide range of contaminants, certain low-abundance or novel contaminants may remain undetected due to spectral overlap or insufficient training data.
(3) Computational Demand: The real-time nature of the system necessitates significant computational resources, which may limit deployment in resource-constrained environments.
(4) Scalability Challenges: While the current configuration processes over 100 tons of RCA per hour, further scaling to larger demolition sites or simultaneous multi-site operations could pose logistical and technical challenges.
(5) Economic Viability: The cost-effectiveness of implementing the system on a large scale, particularly in regions with limited resources, remains to be further assessed.

5.2. Future orientations

To address the limitations and build upon the current findings, the following directions are proposed:

(1) Environmental Adaptability: Developing robust calibration algorithms and protective measures to enhance system performance under diverse environmental conditions, including temperature extremes, high humidity, and airborne particulates.
(2) Enhanced Contaminant Detection: Expanding the spectral database of contaminants using advanced machine learning techniques to improve detection accuracy for rare or emerging contaminants.
(3) Distributed Computing Models: Exploring cloud-based distributed computing solutions to optimize the processing of high-dimensional spectral data, reducing on-site computational burden.
(4) Modular Scalability: Engineering modular systems that can be easily configured for larger-scale or multi-site operations, enabling seamless scalability.
(5) Lifecycle Assessment: Conducting comprehensive cost-benefit and lifecycle assessments to evaluate the economic and environmental impacts of deploying the system at scale.
(6) Integration with Circular Economy Practices: Investigating the integration of real-time RCA data with broader circular economy frameworks to optimize material recovery and reuse in construction projects.
(7) Cross-Disciplinary Applications: Exploring applications of the sensor-based system in other industries such as mining, waste management, and resource recovery, to enhance its versatility and impact.

6. Conclusion

(1) Innovation in Quality Inspection: This study introduces an advanced, mobile sensor-based quality inspection system for RCA, demonstrating its capability to process over 100 tons per hour. The integration of 3D scanning and LIBS provides a comprehensive evaluation of PSD and contaminant detection, setting a new benchmark for non-intrusive RCA quality assessment.
(2) Technological Advancements: By utilizing incremental learning techniques and cloud-based data management, the system ensures continuous model updates without requiring complete retraining. This innovation significantly enhances computational efficiency and sustains high classification performance, addressing the limitations of traditional RCA assessment methods.
(3) Sustainability and Efficiency: The containerized design ensures operational flexibility and enables on-site recycling at demolition sites. This reduces transportation costs, minimizes environmental impact, and aligns with circular economy principles, promoting sustainable construction practices.
(4) Validation and Reliability: Comprehensive validation using X-ray tomography and manual sieving confirms the accuracy of PSD measurements. The Root Mean Square Error values—below 5.5%—highlight the system's robustness in PSD estimation. Similarly, the LIBS sensor's performance was validated under dynamic conditions, demonstrating minimal spectral variation between moving and stationary states of the conveyor belt. The system achieved an accuracy rate of 0.94, a weighted average precision of 0.95, and a weighted F1-score of 0.95 on the validation dataset, underscoring its reliability in real-time contaminant detection. These results collectively affirm the system's high precision and reliability for both PSD and contaminant analysis.
(5) Applications and Impact: The system's adaptability and scalability extend beyond construction to other industries, such as mining and waste management. Its ability to deliver real-time data supports informed decision-making, ensuring consistent material quality and compliance with industry standards.
(6) Future Implications: The demonstrated precision and consistency of LIBS in contaminant detection, even during conveyor motion, underscore its potential for widespread industrial adoption. Incremental learning capabilities provide a foundation for adapting to evolving material compositions, ensuring long-term relevance and applicability.
(7) Contributions to the Field: This research highlights the integration of cutting-edge technologies into RCA processing, bridging the gap between innovation and practical application. It advances the sustainable agenda by harmonizing efficiency and precision, paving the way for eco-friendly infrastructure development without compromising quality standards.

CRediT authorship contribution statement

Cheng Chang: Writing – original draft, Visualization, Validation, Software, Methodology, Investigation, Formal analysis, Data curation, Conceptualization. **Francesco Di Maio:** Writing – review & editing, Supervision, Project administration, Methodology, Funding acquisition, Conceptualization. **Rajeev Bheemireddy:** Software, Data curation. **Perry Posthoorn:** Software, Data curation. **Abraham T. Gebremariam:** Writing – review & editing, Resources. **Peter Rem:** Writing – review & editing, Supervision, Project administration, Methodology, Funding acquisition, Conceptualization.

Fundings

This research was supported by the European Union's Horizon funded Project "Innovative Circular Economy Based solutions demonstrating the Efficient Recovery of valuable material resources from the Generation of representative end-of-life building materials" (ICEBERG, grant agreement No. 869336).

Declaration of competing interest

The authors declare that they have no known competing financial interests or personal relationships that could have appeared to influence the work reported in this paper.

Acknowledgment

The authors acknowledge P.M. Meijvogel-de Koning from the Lab Geoscience and Engineering at Delft University of Technology for her assistance with X-ray tomography.

Data availability

Data will be made available on request.

References

Abdelfattah, A., Costa, T., Dongarra, J., Gates, M., Haidar, A., Hammarling, S., Higham, N.J., Kurzak, J., Luszczek, P., Tomov, S., Zounon, M., 2021. A set of batched basic linear algebra Subprograms and LAPACK routines. ACM Trans. Math Software 47 (3). https://doi.org/10.1145/3431921.

Akhtar, A., Sarmah, A.K., 2018. Construction and demolition waste generation and properties of recycled aggregate concrete: a global perspective. J. Clean. Prod. 186, 262–281. https://doi.org/10.1016/J.JCLEPRO.2018.03.085.

Al Martini, S., Sabouni, R., Khartabil, A., Wakjira, T.G., Shahria Alam, M., 2023. Development and strength prediction of sustainable concrete having binary and ternary cementitious blends and incorporating recycled aggregates from demolished UAE buildings: experimental and machine learning-based studies. Construct. Build. Mater. 380, 131278. https://doi.org/10.1016/J.CONBUILDMAT.2023.131278.

Alaejos, Pilar, de Juan, M.S., Rueda, J., Drummond, R., Valero, I., 2013. Quality assurance of recycled aggregates. In: Vázquez, E. (Ed.), Progress of Recycling in the Built Environment: Final Report of the RILEM Technical Committee 217-PRE. Springer, Netherlands, pp. 229–273. https://doi.org/10.1007/978-94-007-4908-5_6.

Amesho, K.T.T., Chinglenthoiba, C., Samsudin, M.S.A.B., Lani, M.N., Pandey, A., Desa, M.N.M., Suresh, V., 2023. Microplastics in the environment: an urgent need for coordinated waste management policies and strategies. J. Environ. Manag. 344, 118713. https://doi.org/10.1016/j.jenvman.2023.118713.

Aslam, M.S., Huang, B., Cui, L., 2020. Review of construction and demolition waste management in China and USA. J. Environ. Manag. 264, 110445. https://doi.org/10.1016/J.JENVMAN.2020.110445.

Bai, F., Fan, M., Yang, H., Dong, L., 2021. Image segmentation method for coal particle size distribution analysis. Particuology 56, 163–170. https://doi.org/10.1016/J.PARTIC.2020.10.002.

Barri, K., Jahangiri, B., Davami, O., Buttlar, W.G., Alavi, A.H., 2020. Smartphone-based molecular sensing for advanced characterization of asphalt concrete materials. Measurement 151, 107212. https://doi.org/10.1016/J.MEASUREMENT.2019.107212.

Basu, S., Kwee, T.C., Surti, S., Akin, E.A., Yoo, D., Alavi, A., 2011. Fundamentals of PET and PET/CT imaging. Ann. N. Y. Acad. Sci. 1228 (1), 1–18. https://doi.org/10.1111/j.1749-6632.2011.06077.x.

Bobulski, J., Kubanek, M., 2021. Deep learning for plastic waste classification system. Applied Computational Intelligence and Soft Computing 2021 (1), 6626948. https://doi.org/10.1155/2021/6626948.

Bonifazi, G., Palmieri, R., Serranti, S., 2018. Evaluation of attached mortar on recycled concrete aggregates by hyperspectral imaging. Construct. Build. Mater. 169, 835–842. https://doi.org/10.1016/J.CONBUILDMAT.2018.03.048.

Braun, J., Willett, S.D., 2013. A very efficient O(n), implicit and parallel method to solve the stream power equation governing fluvial incision and landscape evolution. Geomorphology 180–181, 170–179. https://doi.org/10.1016/J.GEOMORPH.2012.10.008.

Brunnbauer, L., Gajarska, Z., Lohninger, H., Limbeck, A., 2023. A critical review of recent trends in sample classification using Laser-Induced Breakdown Spectroscopy (LIBS). TrAC, Trends Anal. Chem. 159, 116859. https://doi.org/10.1016/J.TRAC.2022.116859.

Cabral, J.S., Menegatti, C.R., Nicolodelli, G., 2023. Laser-induced breakdown spectroscopy in cementitious materials: a chronological review of cement and concrete from the last 20 years. TrAC, Trends Anal. Chem. 160, 116948. https://doi.org/10.1016/J.TRAC.2023.116948.

Chang, C., 2025. In: Quality Assessment & Monitoring of Recycled Coarse Aggregates.

Chang, C., Di Maio, F., Bheemireddy, R., Posthoorn, P., Gebremariam, A.T., Rem, P., 2025. Rapid quality control for recycled coarse aggregates (RCA) streams: multi-sensor integration for advanced contaminant detection. Comput. Ind. 164, 104196. https://doi.org/10.1016/j.compind.2024.104196.

Chang, C., Maio, F. Di, Rem, P., Gebremariam, A.T., Mehari, F., Xia, H., 2022. Cluster-based identification algorithm for in-line recycled concrete aggregates characterization using Laser-Induced Breakdown Spectroscopy (LIBS). Resour. Conserv. Recycl. 185, 106507. https://doi.org/10.1016/J.RESCONREC.2022.106507.

Chen, T., Zhang, T., Li, H., 2020. Applications of laser-induced breakdown spectroscopy (LIBS) combined with machine learning in geochemical and environmental resources exploration. TrAC, Trends Anal. Chem. 133, 116113. https://doi.org/10.1016/J.TRAC.2020.116113.

Chen, X., Kroell, N., Feil, A., Greiff, K., 2024. Sensor-based sorting. Handbook of Recycling: State-of-the-Art for Practitioners, Analysts, and Scientists 145–159. https://doi.org/10.1016/B978-0-323-85514-3.00028-2.

Dice, L.R., 1945. Measures of the amount of ecologic association between species. Ecology 26 (3), 297–302.

Fajar, A., Sarno, R., Fatichah, C., Fahmi, A., 2022. Reconstructing and resizing 3D images from DICOM files. Journal of King Saud University-Computer and Information Sciences 34 (6), 3517–3526.

Frison, G., Kouzoupis, D., Sartor, T., Zanelli, A., Diehl, M., 2018. BLASFEO: basic linear algebra subroutines for embedded optimization. ACM Trans. Math Software 44 (4). https://doi.org/10.1145/3210754.

Frison, G., Sartor, T., Zanelli, A., Diehl, M., 2020. The BLAS API of BLASFEO: optimizing performance for small matrices. ACM Trans. Math Software 46 (2). https://doi.org/10.1145/3378671.

Fu, Y., Aldrich, C., 2023. Online particle size analysis on conveyor belts with dense convolutional neural networks. Miner. Eng. 193, 108019. https://doi.org/10.1016/J.MINENG.2023.108019.

Galán, B., Viguri, J.R., Cifrian, E., Dosal, E., Andres, A., 2019. Influence of input streams on the construction and demolition waste (CDW) recycling performance of basic and advanced treatment plants. J. Clean. Prod. 236, 117523. https://doi.org/10.1016/j.jclepro.2019.06.354.

Gálvez-Martos, J.L., Styles, D., Schoenberger, H., Zeschmar-Lahl, B., 2018. Construction and demolition waste best management practice in Europe. Resour. Conserv. Recycl. 136, 166–178. https://doi.org/10.1016/J.RESCONREC.2018.04.016.

Hamzeloo, E., Massinaei, M., Mehrshad, N., 2014. Estimation of particle size distribution on an industrial conveyor belt using image analysis and neural networks. Powder Technol. 261, 185–190. https://doi.org/10.1016/J.POWTEC.2014.04.038.

Huber, N., Eschlböck-Fuchs, S., Scherndl, H., Freimund, A., Heitz, J., Pedarnig, J.D., 2014. In-line measurements of chlorine containing polymers in an industrial waste sorting plant by laser-induced breakdown spectroscopy. Appl. Surf. Sci. 302, 280–285. https://doi.org/10.1016/J.APSUSC.2013.10.070.

Huda, W., Slone, R., 1996. Review of radiologic physics. Phys. Med. Biol. 41 (12), 2807.

Kabirifar, K., Mojtahedi, M., Wang, C., Tam, V.W.Y., 2020. Construction and demolition waste management contributing factors coupled with reduce, reuse, and recycle strategies for effective waste management: a review. J. Clean. Prod. 263, 121265. https://doi.org/10.1016/J.JCLEPRO.2020.121265.

Kim, H., Lee, J., Srivastava, E., Shin, S., Jeong, S., Hwang, E., 2021. Front-end signal processing for metal scrap classification using online measurements based on laser-induced breakdown spectroscopy. Spectrochim. Acta B Atom Spectrosc. 184, 106282. https://doi.org/10.1016/J.SAB.2021.106282.

Kim, J., 2022. Influence of quality of recycled aggregates on the mechanical properties of recycled aggregate concretes: an overview. Construct. Build. Mater. 328, 127071. https://doi.org/10.1016/J.CONBUILDMAT.2022.127071.

Lederer, J., Gassner, A., Kleemann, F., Fellner, J., 2020. Potentials for a circular economy of mineral construction materials and demolition waste in urban areas: a case study from Vienna. Resour. Conserv. Recycl. 161, 104942. https://doi.org/10.1016/J.RESCONREC.2020.104942.

Lohumi, S., Cho, B.K., Hong, S., 2021. LCTF-based multispectral fluorescence imaging: system development and potential for real-time foreign object detection in fresh-cut vegetable processing. Comput. Electron. Agric. 180, 105912. https://doi.org/10.1016/J.COMPAG.2020.105912.

Lotfi, S., Di Maio, F., Xia, H., Serranti, S., Palmieri, R., Bonifazi, G., 2015. Assessment of the contaminants level in recycled aggregates and alternative new technologies for contaminants recognition and removal. EMABM 2015: Proceedings of the 15th Euroseminar on Microscopy Applied to Building Materials, pp. 17–19.

Lu, B., Zhou, J., Zhang, Y., Liu, Y., Wang, Q., 2024. An alternative rotating object detection method for rock particle size distribution analysis. Powder Technol. 444, 120059. https://doi.org/10.1016/J.POWTEC.2024.120059.

Luciano, A., Cutaia, L., Altamura, P., Penalvo, E., 2022. Critical issues hindering a widespread construction and demolition waste (CDW) recycling practice in EU countries and actions to undertake: the stakeholder's perspective. Sustainable Chemistry and Pharmacy 29, 100745.

Marie, I., Mujalli, R., 2019. Effect of design properties of parent concrete on the morphological properties of recycled concrete aggregates. Engineering Science and Technology, an International Journal 22 (1), 334–345. https://doi.org/10.1016/J.JESTCH.2018.08.014.

Marín-Cortés, S., Fernández-Álvarez, M., Enríquez, E., Fernández, J.F., 2024. Experimental characterization data on aggregates from construction and demolition wastes for the assistance in sorting and recycling practices. Construct. Build. Mater. 435, 136798. https://doi.org/10.1016/J.CONBUILDMAT.2024.136798.

Marique, A.F., Rossi, B., 2018. Cradle-to-grave life-cycle assessment within the built environment: comparison between the refurbishment and the complete reconstruction of an office building in Belgium. J. Environ. Manag. 224, 396–405. https://doi.org/10.1016/J.JENVMAN.2018.02.055.

Merk, S., Scholz, C., Florek, S., Mory, D., 2015. Increased identification rate of scrap metal using Laser Induced Breakdown Spectroscopy Echelle spectra. Spectrochim. Acta B Atom Spectrosc. 112, 10–15. https://doi.org/10.1016/J.SAB.2015.07.009.

Mewada, D., Agnew, C., Grua, E.M., Eising, C., Denny, P., Heffernan, M., Tierney, K., Van De Ven, P., Scanlan, A., 2024. Contamination detection from highly cluttered waste scenes using computer vision. IEEE Access 12, 129434–129446. https://doi.org/10.1109/ACCESS.2024.3456469.

Nalon, G.H., Santos, R.F., Lima, G. E. S. de, Andrade, I.K.R., Pedroti, L.G., Ribeiro, J.C.L., Franco de Carvalho, J.M., 2022. Recycling waste materials to produce self-sensing concretes for smart and sustainable structures: a review. Construct. Build. Mater. 325, 126658. https://doi.org/10.1016/J.CONBUILDMAT.2022.126658.

Park, S., Lee, J., Kwon, E., Kim, D., Shin, S., Jeong, S., Park, K., 2021. 3D sensing system for laser-induced breakdown spectroscopy-based metal scrap identification. International Journal of Precision Engineering and Manufacturing-Green Technology. https://doi.org/10.1007/s40684-021-00364-1.

Pelc, N.J., 2014. Recent and future directions in CT imaging. Ann. Biomed. Eng. 42, 260–268.

Poon, C.S., Chan, D., 2007. Effects of contaminants on the properties of concrete paving blocks prepared with recycled concrete aggregates. Construct. Build. Mater. 21 (1), 164–175. https://doi.org/10.1016/J.CONBUILDMAT.2005.06.031.

Psarras, C., Barthels, H., Bientinesi, P., 2022. The linear algebra mapping problem. Current state of linear algebra languages and libraries. ACM Trans. Math Software 48 (3). https://doi.org/10.1145/3549935.

Sai Trivedi, S., Snehal, K., Das, B.B., Barbhuiya, S., 2023. A comprehensive review towards sustainable approaches on the processing and treatment of construction and demolition waste. Construct. Build. Mater. 393, 132125. https://doi.org/10.1016/J.CONBUILDMAT.2023.132125.

Sørensen, T.J., 1948. *A Method of Establishing Groups of Equal Amplitude in Plant Sociology Based on Similarity of Species Content and its Application to Analyses of the Vegetation on Danish Commons*. I Kommission Hos E. Munksgaard.

Soto-Paz, J., Arroyo, O., Torres-Guevara, L.E., Parra-Orobio, B.A., Casallas-Ojeda, M., 2023. The circular economy in the construction and demolition waste management: a comparative analysis in emerging and developed countries. J. Build. Eng. 78, 107724. https://doi.org/10.1016/J.JOBE.2023.107724.

Steer, P., Guerit, L., Lague, D., Crave, A., Gourdon, A., 2022. Size, shape and orientation matter: fast and semi-automatic measurement of grain geometries from 3D point clouds. Earth Surf. Dyn. 10 (6), 1211–1232. https://doi.org/10.5194/esurf-10-1211-2022.

Su, Y., Xu, Y., Bao, Z., Ng, S.T., Gao, Q., 2024. Stakeholder interactions of government intervention in construction and demolition waste recycling market: a game theory approach. Developments in the Built Environment 18, 100391. https://doi.org/10.1016/j.dibe.2024.100391.

Trotta, O., Bonifazi, G., Capobianco, G., Serranti, S., 2021. Recycling-oriented characterization of post-earthquake building waste by different sensing techniques. Journal of Imaging 7 (9). https://doi.org/10.3390/JIMAGING7090182.

Tuan, N.M., Kim, Y., Lee, J.-Y., Chin, S., 2022. Automatic stereo vision-based inspection system for particle shape analysis of coarse aggregates. J. Comput. Civ. Eng. 36 (2). https://doi.org/10.1061/(asce)cp.1943-5487.0001005.

Vegas, I., Broos, K., Nielsen, P., Lambertz, O., Lisbona, A., 2015. Upgrading the quality of mixed recycled aggregates from construction and demolition waste by using near-infrared sorting technology. Construct. Build. Mater. 75, 121–128. https://doi.org/10.1016/J.CONBUILDMAT.2014.09.109.

Wang, Z., Afgan, M.S., Gu, W., Song, Y., Wang, Y., Hou, Z., Song, W., Li, Z., 2021. Recent advances in laser-induced breakdown spectroscopy quantification: from fundamental understanding to data processing. TrAC, Trends Anal. Chem. 143, 116385. https://doi.org/10.1016/J.TRAC.2021.116385.

Werheit, P., Fricke-Begemann, C., Gesing, M., Noll, R., 2011. Fast single piece identification with a 3D scanning LIBS for aluminium cast and wrought alloys recycling. J. Anal. Atomic Spectrom. 26 (11), 2166–2174. https://doi.org/10.1039/C1JA10096C.

Wu, H., Liang, C., Zhang, Z., Yao, P., Wang, C., Ma, Z., 2023. Utilizing heat treatment for making low-quality recycled aggregate into enhanced recycled aggregate, recycled cement and their fully recycled concrete. Construct. Build. Mater. 394, 132126. https://doi.org/10.1016/J.CONBUILDMAT.2023.132126.

Wu, L., Sun, Z., Cao, Y., 2024. Modification of recycled aggregate and conservation and application of recycled aggregate concrete: a review. Construct. Build. Mater. 431, 136567. https://doi.org/10.1016/J.CONBUILDMAT.2024.136567.

Xia, H., Bakker, M.C.M., 2014. Reliable classification of moving waste materials with LIBS in concrete recycling. Talanta 120, 239–247. https://doi.org/10.1016/j.talanta.2013.11.082.

Yamazaki, I., Kurzak, J., Wu, P., Zounon, M., Dongarra, J., 2018. Symmetric indefinite linear solver using OpenMP task on multicore architectures. IEEE Trans. Parallel Distr. Syst. 29 (8), 1879–1892. https://doi.org/10.1109/TPDS.2018.2808964.

Zhang, C., Hu, M., Di Maio, F., Sprecher, B., Yang, X., Tukker, A., 2022. An overview of the waste hierarchy framework for analyzing the circularity in construction and demolition waste management in Europe. Sci. Total Environ. 803, 149892. https://doi.org/10.1016/J.SCITOTENV.2021.149892.

Zhang, K., Qing, Y., Umer, Q., Asmi, F., 2023. How construction and demolition waste management has addressed sustainable development goals: Exploring academic and industrial trends. J. Environ. Manag. 345, 118823.

Zhang, Z., Liu, Y., Hu, Q., Zhang, Z., Wang, L., Liu, X., Xia, X., 2020. Multi-information online detection of coal quality based on machine vision. Powder Technol. 374, 250–262. https://doi.org/10.1016/J.POWTEC.2020.07.040.